Export of nutrients from the Arctic Ocean

Sinhué Torres-Valdés,[1] Takamasa Tsubouchi,[2] Sheldon Bacon,[2]
Alberto C. Naveira-Garabato,[3] Richards Sanders,[1] Fiona A. McLaughlin,[4] Brian Petrie,[5]
Gerhard Kattner,[6] Kumiko Azetsu-Scott,[5] and Terry E. Whitledge[7]

Received 16 March 2012; revised 4 October 2012; accepted 15 December 2012; published 3 April 2013.

[1] This study provides the first physically based mass-balanced transport estimates of dissolved inorganic nutrients (nitrate, phosphate, and silicate) for the Arctic Ocean. Using an inverse model-generated velocity field in combination with a quasi-synoptic assemblage of hydrographic and hydrochemical data, we quantify nutrient transports across the main Arctic Ocean gateways: Davis Strait, Fram Strait, the Barents Sea Opening (BSO), and Bering Strait. We found that the major exports of all three nutrients occur via Davis Strait. Transports associated with the East Greenland Current are almost balanced by transports associated with the West Spitsbergen Current. The most important imports of nitrate and phosphate to the Arctic occur via the BSO, and the most important import of silicate occurs via Bering Strait. Oceanic budgets show that statistically robust net silicate and phosphate exports exist, while the net nitrate flux is zero, within the uncertainty limits. The Arctic Ocean is a net exporter of silicate (-15.7 ± 3.2 kmol s^{-1}) and phosphate (-1.0 ± 0.3 kmol s^{-1}; net $\pm$ 1 standard error) to the North Atlantic. The export of excess phosphate (relative to nitrate) from the Arctic, calculated at -1.1 ± 0.3 kmol s^{-1}, is almost twice as large as previously estimated. Net transports of silicate and phosphate from the Arctic Ocean provide 12% and 90%, respectively, of the net southward fluxes estimated at 47°N in the North Atlantic. Additional sources of nutrients that may offset nutrient imbalances are explored, and the relevance and the pathway of nutrient transports to the North Atlantic are discussed.

Citation: Torres-Valdés, S., T. Tsubouchi, S. Bacon, A. C. Naveira-Garabato, R. Sanders, F. A. McLaughlin, B. Petrie, G. Kattner, K. Azetsu-Scott, and T. E. Whitledge (2013), Export of nutrients from the Arctic Ocean, *J. Geophys. Res. Oceans*, *118*, 1625–1644, doi:10.1002/jgrc.20063.

1. Introduction

[2] While oceanic nutrient inputs to the Arctic Ocean are associated with waters of Pacific and Atlantic origin, important riverine nutrient fluxes to the upper layers of the Arctic Ocean also originate in the watersheds surrounding it. Current changes in the hydrological cycle at high latitudes have resulted in increased runoff into the Arctic Ocean [*McClelland et al*., 2006; *Peterson et al*., 2002; *Peterson et al*., 2006; *Shiklomanov and Lammers*, 2009], with associated changes in the quality and quantity of the nutrients supplied from these watersheds [*Frey and McClelland*, 2009; *Frey et al*., 2007; *Raymond et al*., 2007]. River loads of silicate, phosphate, and dissolved and particulate organic matter are expected to increase as rising temperatures impact the permafrost around the Arctic rim [*Frey and McClelland*, 2009]. However, the future trend in riverine nitrogen loads is unclear [*Frey and McClelland*, 2009], or expected to drop [*Bouwman et al*., 2005].

[3] In open waters of the Arctic Ocean, primary production has increased as a result of the long-term trend reduction in the summer sea-ice cover [*Arrigo et al*., 2008; *Pabi and Arrigo*, 2008], with associated enhanced export of biogenic particulate carbon [e.g., *Lalande et al*., 2009a, 2009b]. Even so, most of the export production in the Arctic is remineralised at shallow depths [*Anderson et al*., 2003; *Cai et al*., 2010; *Honjo et al*., 2010; *Macdonald et al*., 2010], thereby implying that all—or a proportion—of the river and oceanic nutrient inputs to the upper layers of the Arctic must be exported to the North Atlantic. The ultimate fate of nutrients is of wider relevance as they can potentially support primary production elsewhere.

[4] There are only a few studies available where nutrient transports and budgets have been estimated in the Arctic. Mass balance calculations indicate that silicate is balanced in the Arctic Ocean, implying silica burial in the system is negligible [*Anderson et al.*, 1983; *Jones and Coote*, 1980].

[1]Ocean Biogeochemistry and Ecosystems, National Oceanography Centre, Southampton, Southampton, UK.
[2]Marine Physics and Ocean Climate, National Oceanography Centre, Southampton, Southampton, UK.
[3]Ocean and Earth Science, University of Southampton, Water Front Campus, National Oceanography Centre, Southampton, Southampton, UK.
[4]Institute of Ocean Sciences, Fisheries and Oceans Canada, Sidney, British Columbia, Canada.
[5]Department of Fisheries and Oceans, Bedford Institute of Oceanography, Dartmouth, Nova Scotia, Canada.
[6]Alfred Wegener Institute for Polar and Marine Research, Bremerhaven, Germany.
[7]Institute of Marine Science, School of Fisheries and Ocean Sciences, University of Alaska Fairbanks, Fairbanks, Alaska, USA.

Corresponding author: S. Torres-Valdés, Ocean Biogeochemistry and Ecosystems, National Oceanography Centre, Southampton, European Way SO14 3ZH, Southampton, UK. (sinhue@noc.ac.uk)

2169-9275/13/10.1002/jgrc.20063

There have not been similar budget estimates for phosphate and nitrate, although a transport of excess phosphate (2×10^{10} mol yr^{-1} ≈ 0.63 kmol s^{-1}) via the Arctic throughflow has been estimated by *Yamamoto-Kawai et al.* [2006]. The relevance of this excess phosphate transport is that it could potentially supply 23% of the phosphorus demand for nitrogen fixation in the North Atlantic. In a recent biogeochemical budget study for the Arctic Ocean, *Macdonald et al.* [2010] estimated that the Arctic Ocean imports ~42.5 kmol nitrogen s^{-1}, 3.9 kmol phosphorus s^{-1}, and 32 kmol silicate s^{-1} from the Pacific and Atlantic Oceans, but these are lower than their estimates of new production over the Arctic shelves, implying that other sources exist. *Macdonald et al.* [2010] also pointed out that riverine loads of nitrogen cannot account for the losses of nitrogen via denitrification, which in the Arctic has been estimated to remove between ~14 and 66 kmol N s^{-1} [*Chang and Devol*, 2009].

[5] Despite the potential importance of nutrient transports for primary production in the Arctic or elsewhere and the ongoing hydrological changes at high latitudes and associated modification of nutrient inputs, there are still no available estimates of nutrient transports across the Arctic Ocean boundaries that make use of simultaneous measurements of hydrography and hydrochemistry. In this study, we aimed to compute oceanic transports of dissolved inorganic nutrients (nitrate, phosphate, and silicate) across the main Arctic Ocean gateways—Davis Strait, Fram Strait, the Barents Sea Opening (BSO), and Bering Strait—and to determine whether nutrient imbalances exist. We combine recent nutrient sections with velocity fields generated with an inverse model recently developed to estimate heat and freshwater fluxes [*Tsubouchi et al.*, 2012, referred to hereafter as T2012]. We compare our results with previous nutrient transport estimates and discuss the origin of budget imbalances and the fate of nutrient fluxes downstream.

2. Methods and Data

[6] Nutrient transports were computed by combining an inverse model-generated velocity field with optimally interpolated nutrient data from hydrographic sections around the Arctic Ocean (Figure 1). In this section, we first briefly describe the inverse model structure, the resulting velocity field, and the water mass boundaries considered in the model.

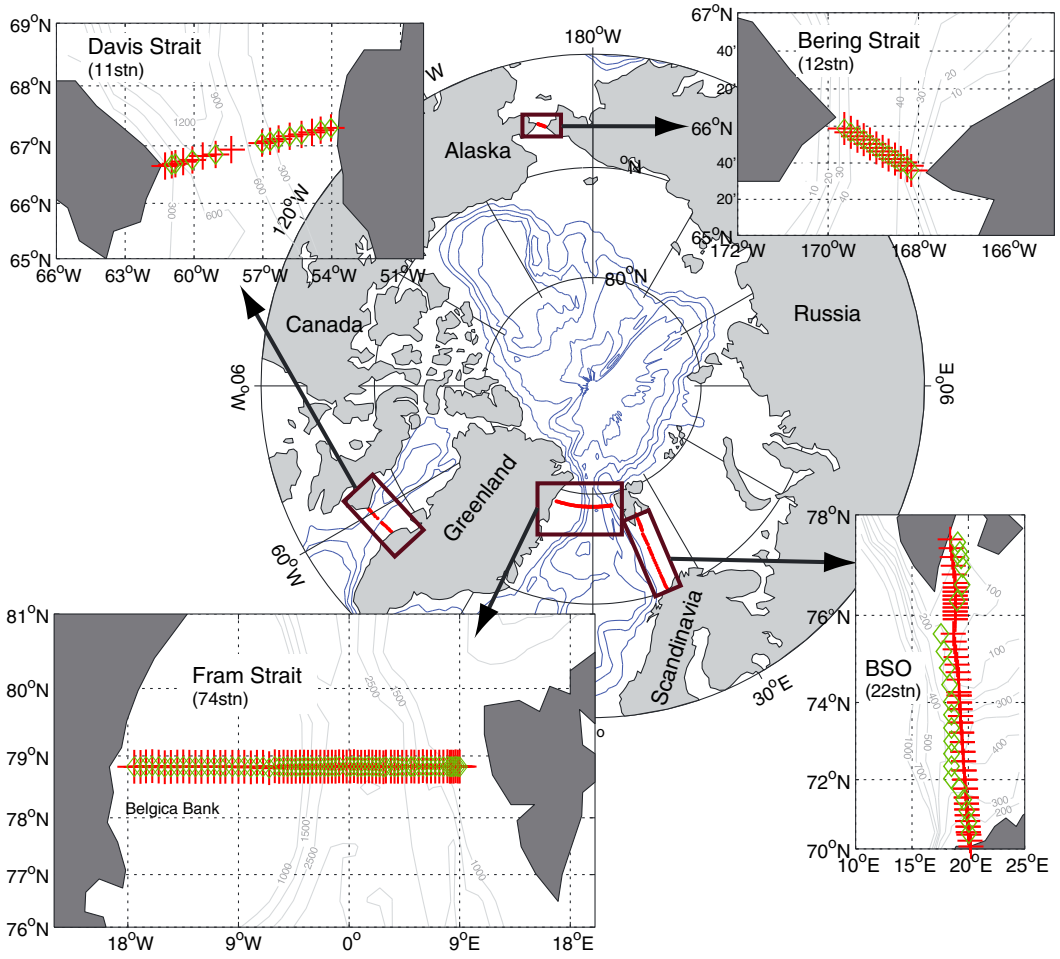

Figure 1. Map of the Arctic Ocean showing station pair locations (red crosses) and hydrochemical data stations (green diamonds) across the main four gateways considered in this study: Davis Strait, Fram Strait, Barents Sea Opening (BSO), and Bering Strait. Number of stations per gateway is indicated. Depth contours are shown for reference.

For a fuller description of the inverse model and hydrographic data used, the reader is referred to T2012. Second, we document the hydrochemical data used, and briefly describe the main features of the nutrient distributions. Third, we set out the approach undertaken to compute nutrient transports and to generate oceanic nutrient budgets.

2.1. Model Structure, Velocity Field, and Water masses

[7] The model is based on the steady geostrophic box inversions described by *Wunsch* [1996], and it represents the Arctic Ocean as a single 15 layered box with the layers defined by isopycnal surfaces (Figure 2a). There are four main gateways around the Arctic Ocean: Davis Strait, Fram Strait, the BSO, and Bering Strait. An optimal horizontal velocity field across these boundaries is generated based on hydrographic data collected in summer 2005 during a 32 day period. This is believed to be a representative equilibrium oceanic circulation field for summer 2005 which conserves volume and salinity transports, including sea ice and net surface freshwater fluxes, and also generates estimates of the diapycnal velocity field in the Arctic Ocean interior, sea ice volume flux in Fram Strait, and Arctic Ocean net surface heat and fresh water fluxes. The model does not include transports through the small Fury and Hecla Strait, for which adequate data is not available. This deficiency is treated as an uncertainty of 0.05 Sv ($1\ \mathrm{Sv} = 10^6\ \mathrm{m^3\ s^{-1}}$) in seawater transport and 5 mSv in freshwater transport in the model (see T2012 for detailed discussion).

[8] Figure 2b shows the horizontal velocity field obtained by T2012. It captures a conventional circulation field that includes the inflow branches of the West Spitsbergen Current (WSC) located on the eastern side of Fram Strait (3.8 ± 1.3 Sv), Atlantic Water (AW) inflows via the central part of the BSO (2.6 ± 0.9 Sv), and Bering Strait Pacific Water inflows (1.0 ± 0.2 Sv). For the Arctic outflow branches, the East Greenland Current (EGC) is located in the western side of Fram Strait (5.4 ± 2.1 Sv), while a fresher outflow exits via Davis Strait (3.1 ± 0.7 Sv). The total cumulative horizontal ocean volume transport around the Arctic Ocean boundary reveals a 0.14 Sv deficit plus sea ice export via Fram Strait of 0.05 Sv, which are balanced by a surface freshwater input of 0.19 Sv [T2012].

[9] Water masses are typically defined in potential temperature/salinity (θ-S) space; hence, there is no unique relationship between them and layers defined by density. The model upon which this study is based uses a simple but useful definition of water masses to provide a nutrient transport study which is physically consistent with the heat and freshwater transports in T2012. Here, we briefly describe the water mass distribution around the main gateways to provide context for the nutrient distributions and transport computations. The water mass terminology in the descriptions

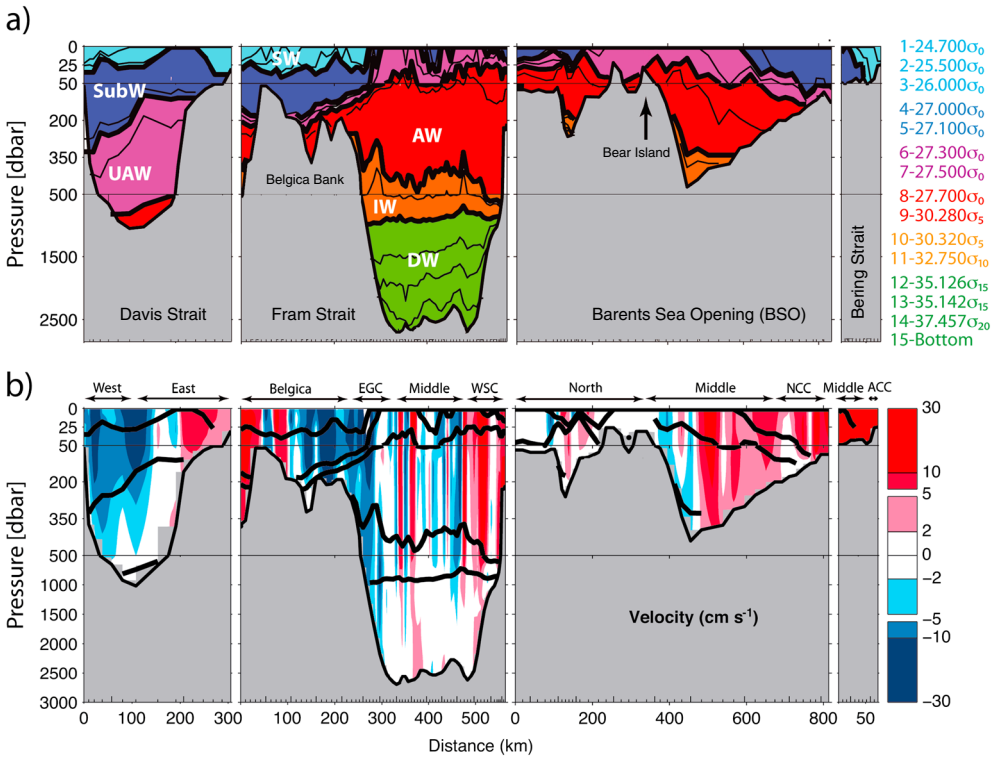

Figure 2. (a) Water mass distributions and (b) inverse model velocity section across the main Arctic Ocean gateways. Velocity units are in cm s^{-1}; negative indicates outputs and positive indicates inputs. From left to right: Davis Strait, Fram Strait, BSO, and Bering Strait. Water masses and associated isopycnal layers are Surface Water (SW, layers 1–3), Subsurface Water (SubW, layers 4–5), Upper Atlantic Water (UAW, layers 6–7), Atlantic Water (AW, layers 8–9), Intermediate Water (IW, layers 10–11), Deep Water (DW, layers 12–15). Isopycnal reference layers are also shown. Note depth scale is expanded from 0–50, 50–500, and 500–3000 m. Approximate locations of the Norwegian and Alaskan Coastal Currents (NCC, ACC) are indicated.

below is related to the principal water masses present in the Arctic Ocean. This information as well as the main considerations for selected water masses in the model and their physical characteristics are detailed in the text and Table 1 in T2012.

[10] Figure 2a shows that surface (SW) and subsurface (SubW) waters are mainly found in the upper 200 m of the water column across Davis Strait and across the Belgica Bank on the Fram Strain section. SubW is mostly found in the southernmost part of the BSO, and both SubW and SW occupy Bering Strait in similar proportions. Upper Atlantic Water (UAW) occupies almost half of Davis Strait and it is also present as a thin layer of ~50 m thickness across the Belgica Bank, gradually shoaling from 200 m deep at distance 0 km of the section and outcropping at distance 300 km. UAW is present all across the BSO, occupying most of the upper 50 m between distance 200 to 600 km, then deepening towards the end of the section. AW occupies a large proportion of the upper 500 m of the water column across Fram Strait and the BSO. A small proportion of this water is present at the deepest part of Davis Strait. Across Fram Strait, the AW layer increases in thickness from west to east. It is shallower in the north part of the BSO and deeper in the south of the section. Intermediate Water (IW) is present underlying the AW and can be seen as a layer thinning from west to east between the depths of ~350 and 800 m across Fram Strait. This water is also present at the bottom of the BSO south and north of Bear Island. Finally, Deep Water (DW) occupies most of Fram Strait from about 800 m down to the bottom.

2.2. Hydrochemical Data

[11] Nitrate + nitrite (hereafter referred to as nitrate), phosphate, and silicate data for the four gateways were obtained from cruises conducted in summer 2005, supplemented with data from summers of other years (Figure 1). Data from Davis Strait were collected in September 2005 as part of the Freshwater Initiative undertaken by the Applied Physics Laboratory (University of Washington) and Bedford Institute of Oceanography [*Lee et al*., 2004]. Samples were collected, frozen, and later analyzed using a Technicon Autoanalyser following World Ocean Circulation Experiment procedures [*Gordon et al*., 1993]. Analytical precisions were <1%–2% for silicate and nitrate, and <1%–3% for phosphate. Data from Fram Strait were collected as part of the ARK-XXI 1b expedition from 16 August to 9 September 2005 [*Budéus et al*., 2008; *Kattner*, 2009]. Seventy-seven conductivity-temperature-depth stations were occupied across Fram Strait (78.8°N, 8.9°E–17.5°W), and nutrient measurements were carried out on board using an Evolution III (Alliance Instruments, France) autoanalyzer based on slightly modified manual methods [*Grasshoff et al*., 1999] and automated techniques [*Aminot et al*., 2009] for seawater analyses. Data from the BSO in April (north of Bear Island) and June (south of Bear Island) 2002 were obtained via the International Council for the Exploration of the Sea Oceanographic Database at http://ices.dk/ocean. Finally, nutrient data from Bering Strait were collected between 17–24 August 2005 as part of the Joint Russian-American Long-Term Census of the Arctic program (http://www.arctic.noaa.gov/aro/russian-american/). All sections were optimally interpolated [*Roemmich*, 1983] on pressure, vertically and horizontally at intervals matching station pair locations (Figure 1).

2.3. Nutrient Distributions

[12] Figure 3 shows optimally interpolated nutrient fields across the four major Arctic Ocean gateways. Overall, the vertical structure of the nutrient fields shows typical distributions, with (1) low concentrations in the upper sunlit layers likely due to utilization of nutrients during primary production and (2) concentrations increasing with depth due to remineralization and/or dissolution of sinking particles. A striking feature, common to all three nutrients, is the elevated concentrations in Davis Strait and Bering Strait compared to the concentrations across Fram Strait and the BSO at similar depths. Highest nutrient concentrations at depths ≤50 m occur on the western side of Bering Strait (>17 μmol-nitrate L^{-1}, >1.5 μmol-phosphate L^{-1}, and 35 μmol-silicate L^{-1}), while at depths between 350 and 1000 m, the highest concentrations (reaching up to 17 μmol-nitrate L^{-1}, 1.5 μmol-phosphate L^{-1}, and 35 μmol-silicate L^{-1}) occur in Davis Strait associated with Upper Atlantic Water and Atlantic water. Elevated nitrate concentrations (~12 μmol L^{-1}) also occur across Fram Strait and the BSO below ~350 m.

2.4. Nutrient Transport Calculations

[13] Horizontal oceanic nutrient transports (T_n; kmol s^{-1}) were calculated from the velocity field and hydrochemical data as follows:

$$T_n = \sum_{j=1}^{N} \Delta x_j \int_{bottom}^{surface} v_j c_j dz \quad (1)$$

[14] where j is the station pair index and Δx_j represents station pair spacing (m). For each station pair j, $v_j = v_j(z)$ is the velocity (m s^{-1}) profile for station j, and $c_j = c_j(z)$ is the nutrient concentration (μmol L^{-1}) profile. Thus, equation 1 expresses the summation of horizontal transports per station pair integrated from the maximum observation depth up to the sea surface across the pan-Arctic boundary.

3. Transports and Uncertainties

3.1. Oceanic Nutrient Transports

[15] To identify major inputs to and outputs from the Arctic Ocean, the cumulative transports eastward from the westernmost data point in Davis Strait to the easternmost data point in Bering Strait are presented (Figures 4 and 5). Transports are also presented as full integrals per gateway and per components of each gateway in Table 1. Components are also indicated in figures for reference. For explanatory purposes, nutrient transports will be referred to as nitrate (kmol-N s^{-1}), phosphate (kmol-P s^{-1}), and silicate (kmol-Si s^{-1}). We now discuss each strait in sequence.

[16] *Davis Strait*: Major nutrient transports from the Arctic Ocean to the North Atlantic occur via Davis Strait (−31 kmol-N s^{-1}, −4 kmol-P s^{-1}, and −43 kmol-Si s^{-1}). Most of the outflow occurs across the western side of Davis Strait, driven mainly by UAW (−1.5 Sv) and SubW (−2.0 Sv). These two water masses, respectively, yield nutrient transports of −20 and −18 kmol-N s^{-1}, −2.0 and −2.4 kmol-P s^{-1}, and −25 and −24 kmol-Si s^{-1}. The total northward transport of volume (0.9 Sv) and nutrients (6, 0.7, and 5.6 kmol s^{-1} of

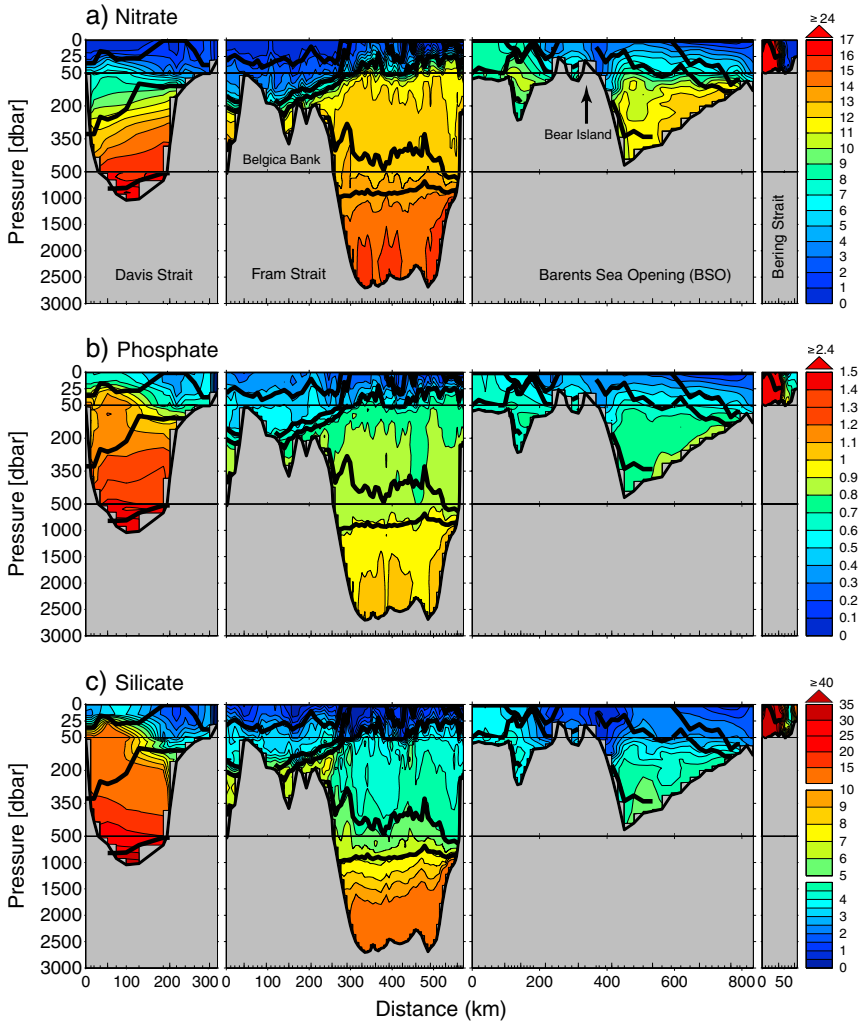

Figure 3. Nutrient sections across the main Arctic Ocean gateways. (a) Nitrate, (b) phosphate, and (c) silicate. Color bars show nutrient concentrations in μmol L^{-1}. Data used were collected during the summer: Davis Strait (September 2005), Fram Strait (August–September 2005), BSO (April and June 2002), and Bering Strait (August 2005). Note depth scale is expanded from 0–50, 50–500, and 500–3000 m.

N, P, and Si, respectively) into Baffin Bay via the eastern side of Davis Strait is much too small to offset the outflow.

[17] *Fram Strait*: Net transports indicate that Fram Strait is a comparatively smaller exporter of nutrients, supplying −10 kmol-N s^{-1}, −0.9 kmol-P s^{-1}, and −7 kmol-Si s^{-1} to the Greenland Sea. Total nutrient inputs toward the central part of Belgica Bank are small (∼9 kmol-N s^{-1}, ∼1 kmol-P s^{-1}, and ∼5 kmol-Si s^{-1}) and are offset toward the eastern edge, such that the total cumulative transports up to Belgica Bank are similar to those at Davis Strait. Along the deepest part of Fram Strait, the large volume and nutrient outflow associated with the EGC (−5.4 Sv, −63 kmol-N s^{-1}, −4.4 kmol-P s^{-1}, and −34 kmol-Si s^{-1}) is almost balanced by the inflow associated with the WSC and the minor inputs across the middle section, making up 4 Sv, 52 kmol-N s^{-1}, 3.5 kmol-P s^{-1}, and 27 kmol-Si s^{-1}. However, most of the transport across Fram Strait is supported by the recirculating deep waters, with ∼3.6 Sv, ∼53 kmol-N s^{-1}, ∼3.5 kmol-P s^{-1}, and ∼27 kmol-Si s^{-1} in the EGC, and ∼1.7 Sv, ∼25 kmol-N s^{-1}, ∼1.7 kmol-P s^{-1}, and ∼15 kmol-Si s^{-1} in the WSC (Figures 4 and 5, DW and IW).

[18] *BSO*: Important inputs of nutrients to the Arctic Ocean occur via the BSO: ∼34 kmol-N s^{-1}, 2.4 kmol-P s^{-1}, and 13 kmol-Si s^{-1}. Transports north of Bear Island (0.2 Sv, 2 kmol-N s^{-1}, 0.1 kmol-P s^{-1}, and 0.8 kmol-Si s^{-1}) and those associated with the Norwegian Coastal Current (0.8 Sv, 5 kmol-N s^{-1}, 0.4 kmol-P s^{-1}, and 1.9 kmol-Si s^{-1}) are small. The main influx is found across the middle part of the BSO (2.7 Sv, ∼27 mol-N s^{-1}, ∼2 kmol-P s^{-1}, and ∼10 kmol-Si s^{-1}), mainly associated with the AW layer.

[19] *Bering Strait*: The largest inputs of silicate (∼21 kmol s^{-1}) occur via Bering Strait, which derives from the high nutrient content in waters of Pacific origin. Nitrate (9 kmol s^{-1}) and phosphate (1.3 kmol s^{-1}) inputs to the Arctic Ocean across Bering Strait are smaller than those across the BSO, but they are comparable to the outputs occurring across the much deeper Fram Strait.

[20] In summary, what we see here is that (1) the major exports of all nutrients to the North Atlantic occur via Davis Strait; (2) transports associated with the EGC are almost balanced by the opposing transports associated with the WSC across Fram Strait, where most of the transport is

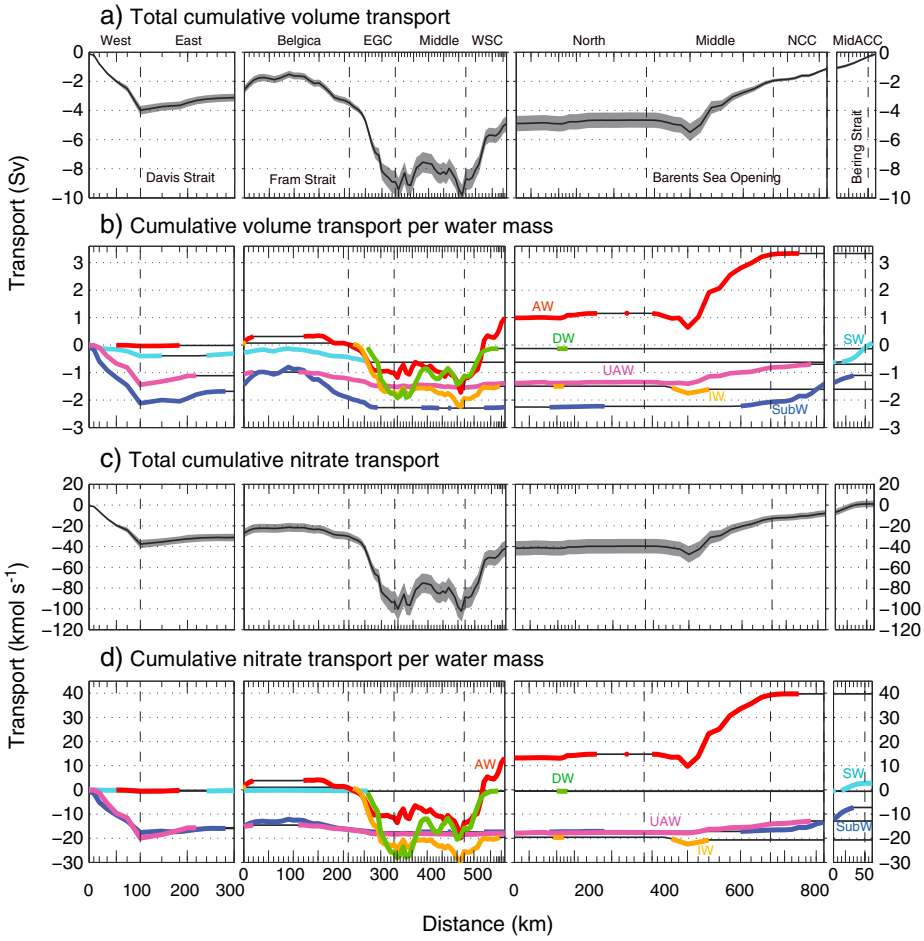

Figure 4. Cumulative transports: (a) total cumulative volume transport, (b) cumulative transport per water mass, (c) total cumulative nitrate transport, and (d) cumulative nitrate transport per water mass. Grey-shaded uncertainty bands (±1 standard deviation) are shown in Figures 4a and 4c (details given in section 3.2). Volume transport is given in Sv and nitrate transports in kmol s^{-1}. Line colors represent full depth transport (black), surface layer (light blue), subsurface layer (dark blue), upper Atlantic Water layer (purple), Atlantic Water layer (red), Intermediate Water layer (yellow), and deep water layer (green). Components per section are indicated in the top panel for reference as per Table 1.

supported by the locally recirculating DW and IW; (3) the most important imports of nitrate and phosphate to the Arctic Ocean occur via the BSO, while (4) the most important imports of silicate occur via Bering Strait; (5) total nitrate imports are slightly larger than total outputs, resulting in a net inflow 1 kmol-N s^{-1}, but in the case of phosphate and silicate, exports are larger than imports, yielding net exports from the Arctic Ocean of −1.0 kmol-P s^{-1} and −15.7 kmol-Si s^{-1}.

3.2. Transport Uncertainties

[21] We have quantified nutrient transports across the four main Arctic Ocean Gateways (Davis, Fram, and Bering Straits, and the BSO) using a near-synoptic summer 2005 velocity field combined with an assembly of hydrochemical data, most of which are from summer 2005. Given spatial and temporal variability in all parameters, we now wish to assess the robustness of our nutrient transports. Two factors control oceanic nutrient transport uncertainty: volume transport variability and nutrient concentration variability. Nutrient transport uncertainty will be determined via multiple nutrient transport calculations spanning the range of volume transport and nutrient concentration uncertainties in combination.

[22] First, we examine the volume transport variability in summer 2005. In order to generate alternative velocity fields representative of a posteriori velocity uncertainty, it is necessary to adopt a procedure that retains total conservation of volume and salinity [T2012]. Most of the Arctic boundary transports are borne by five currents: in Davis Strait (export), the EGC (export), the WSC (import), the BSO (import), and Bering Strait (import). A modified set of velocity fields is prepared, starting with the standard velocity field, by varying these five currents one by one. The applied perturbation is a change of volume transport by its three-month standard deviation (both positive and negative), as observed by moored current meters [T2012], assuming that the variability is barotropic. Volume and salinity conservation are then re-imposed by running a box-inverse model with two constraints: full depth volume and salinity conservation. This process generates 10 different velocity fields, one "high" and one "low" for each of the five currents (Figure 4a).

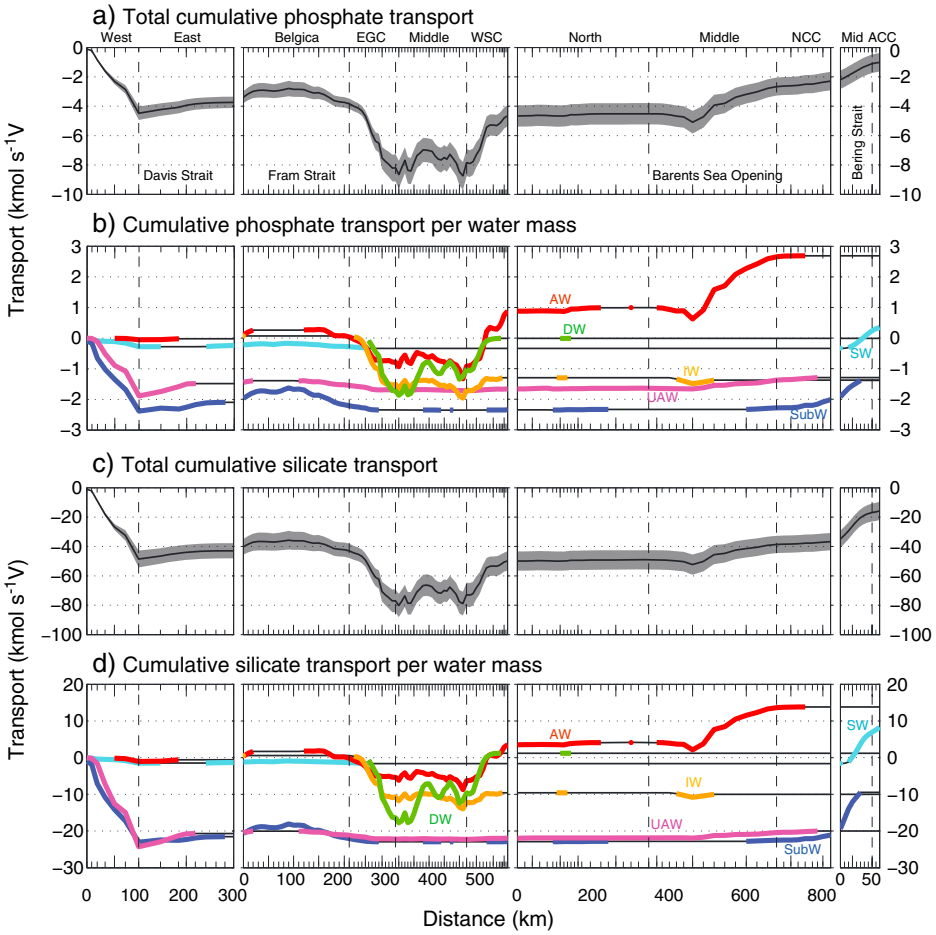

Figure 5. Cumulative transports: (a) total cumulative phosphate transport, (b) cumulative phosphate transport per water mass, (c) total cumulative silicate transport, and (d) cumulative silicate transport per water mass. Grey-shaded uncertainty bands (±1 standard deviation) are shown in Figures 5a and 5c (details given in section 3.2). Volume transport is given in Sv and nutrient transports in kmol s^{-1}. Line colors and indicated gateway components as in Figure 4.

[23] Second, we consider the nutrient concentration variability, which we wish to examine in summer 2005. However, the necessary measurements do not exist. As an alternative, we examine instead the summer nutrient concentration data from different years. The alternative (or "secondary") section is assembled using data from Davis Strait (September 2004), Fram Strait (September 1998), the BSO (September 2003) (when data is only available south of Bear Island), and Bering Strait (July 2005) (when data is only available on the US side of Bering Strait). The difference between the primary and secondary sections is shown in Figure 6. Differences exist mainly in the upper 200 m of the water column, ranging from ~2 to 10 μmol L^{-1} nitrate, ~ 0.2–1 μmol L^{-1} phosphate, and ~ 2–10 μmol L^{-1} silicate (Figure 6). Six alternative nutrient distributions are created using the primary section, the secondary section, and then swapping one at a time one of the four gateways from the secondary section into the primary section.

[24] Finally, 66 possible nutrient transports are calculated using all combinations of 11 velocity sections (the standard, plus five each "high" and "low") and 6 nutrient sections. Table 1 shows the best estimate of nutrient transports, resulting from the combination of the standard velocity field with the primary nutrient section; the standard deviation is derived from the 66 permutations of nutrient transports. Figures 4 and 5 show the cumulative transports (with standard deviations) of nutrients across the Arctic boundary. Phosphate and silicate net transports are -1.0 ± 0.6 and -15.7 ± 6.3 kmol s^{-1}, respectively. Conversion from standard deviation to standard error of the mean, to assess significance of non-zero net transport, requires knowledge of the number of degrees of freedom in the nutrient transports. The most brutal (minimal) assessment of this number is 4: one velocity field, plus its standard deviation, plus two nutrient fields. The phosphate and silicate standard errors are then 0.3 and 3.2 kmol s^{-1}, respectively; therefore, the phosphate and silicate net transports are both significantly different from zero. With a standard error of 1.6 kmol s^{-1}, the net nitrate transport of 1.0 kmol s^{-1} is not significantly different from zero.

3.3. Summary of Results

[25] Our results are consistent with current knowledge [e.g., *Anderson et al.*, 1983; *Tremblay et al.*, 2002a; *Codispoti*

Table 1. Volume and Nutrient Transports Through the Four Arctic Gateways, per Component of Each Gateway and Through Fram Strait Above the Deep Water (DW)[a]

Gateways	Volume (±*SD*, Sv)	Nitrate (±*SD*, kmol s^{-1})	Phosphate (±*SD*, kmol s^{-1})	Silicate (±*SD*, kmol s^{-1})	P^*[b]
Davis Strait	−3.1 ± 0.3	−31.3 ± 3.6	−3.7 ± 0.4	−42.9 ± 5.2	−1.8 ± 0.2
Fram Strait	−1.8 ± 0.6	−10.3 ± 7.5	−0.9 ± 0.8	−7.0 ± 5.9	−0.3 ± 0.5
BSO	3.8 ± 0.5	33.6 ± 5.1	2.4 ± 0.4	13.2 ± 2.1	0.3 ± 0.1
Bering Strait	1.0 ± 0.1	9.0 ± 0.8	1.3 ± 0.1	20.9 ± 2.4	0.7 ± 0.1
Total[c]	−0.14 ± 0.0	1.0 ± 3.2	−1.0 ± 0.6	−15.7 ± 6.3	−1.1 ± 0.5
• *Davis Components*					
West	−4.0 ± 0.3	−37.6 ± 4.0	−4.5 ± 0.5	−48.5 ± 5.8	−2.1 ± 0.3
East	0.9 ± 0.1	6.3 ± 1.2	0.7 ± 0.1	5.6 ± 1.4	0.3 ± 0.1
• *Fram Components*					
Belgica Bank	−0.4 ± 0.1	1.0 ± 0.7	−0.1 ± 0.4	−0.0 ± 0.8	−0.2 ± 0.1
East Greenland Current (EGC)	−5.4 ± 0.9	−63.2 ± 11.5	−4.4 ± 1.0	−34.1 ± 8.1	−0.4 ± 0.6
Middle	0.2 ± 0.6	4.9 ± 8.6	0.3 ± 0.6	4.3 ± 5.2	0.0 ± 0.1
West Spitsbergen Current (WSC)	3.8 ± 0.7	46.9 ± 8.6	3.2 ± 0.6	22.8 ± 4.9	0.3 ± 0.1
• *BSO Components*					
North	0.2 ± 0.0	2.0 ± 0.4	0.1 ± 0.0	0.8 ± 0.1	0.0 ± 0.0
Middle	2.7 ± 0.4	26.7 ± 4.4	1.9 ± 0.3	10.5 ± 1.8	0.2 ± 0.1
Norwegian Coastal Current (NCC)	0.8 ± 0.1	4.9 ± 0.9	0.4 ± 0.1	1.9 ± 0.3	0.1 ± 0.0
• *Bering Components*					
Main	0.8 ± 0.1	9.0 ± 0.8	1.2 ± 0.1	19.6 ± 2.1	0.6 ± 0.0
Alaskan Coastal Current (ACC)	0.2 ± 0.0	0.0 ± 0.0	0.1 ± 0.0	1.3 ± 0.3	0.1 ± 0.0
Fram Strait Above DW					
Fram Strait total	−1.7 ± 0.4	−9.8 ± 5.0	−0.9 ± 0.6	−8.2 ± 4.6	−0.3 ± 0.4
EGC	−3.6 ± 0.6	−38.0 ± 6.6	−2.7 ± 0.7	−18.1 ± 5.3	−0.3 ± 0.4
Middle	0.5 ± 0.2	−5.0 ± 2.6	−0.3 ± 0.2	−2.3 ± 1.1	0.0 ± 0.0
WSC	2.8 ± 0.4	32.2 ± 4.5	2.2 ± 0.3	12.3 ± 2.1	0.2 ± 0.1

[a]The uncertainties shown are the result of the sensitivity analysis described in section 3.2. Positive values indicate inputs to the Arctic Ocean and negative values indicate outputs from the Arctic Ocean.
[b]P^* is discussed in section 4.3.
[c]Note that the total is not the result of adding up transports through the different gateways but the result of the integral across all gateways.

et al., 2009], showing that Bering Strait is an important conduit of nutrients to the upper layers of the Arctic Ocean on the Pacific sector, in particular of silicate. New to the previous transport estimates is not only the inclusion of nitrate and phosphate but also the transport calculations across the BSO. Examination of Figures 4 and 5 reveals the character of circum-Arctic nutrient fluxes. Common to all three nutrients is the domination of the export flux by Davis Strait, specifically by the Labrador Current in the west of the Davis Strait. Fram Strait is seen to be a minor contributor to net fluxes; it supports a small net export, contained within which is a large recirculation dominated by the Deep Water. For the remaining two gateways, the picture changes somewhat. For nitrate, the import balancing the Davis Strait export is found in the BSO, with a small import in Bering Strait which is similar in magnitude to the small Fram Strait export. For phosphate, again there is a modest Bering Strait import similar to the Fram Strait export, but now while the BSO supports the major import flux, it is insufficient to balance the Davis Strait export, leaving a significant net export of phosphate. Finally, looking at silicate, we now see that the small Fram Strait export is nearly balanced by the small BSO import; the major import flux occurs in Bering Strait, but this only accounts for about half of the Davis Strait export, leaving a substantial and significant net Arctic export of silicate. The key messages are (1) the major import fluxes of nitrate and phosphate occur in the BSO, while the major import flux of silicate occurs in Bering Strait; (2) the major export fluxes of nitrate, phosphate, and silicate all occur via Davis Strait.

4. Discussion

4.1. Comparison with previous studies

4.1.1. Arctic Ocean Volume Transport Budget Structure

[26] Having presented the oceanic nutrient transports and budgets, and the robustness of the calculations, we now wish to compare our study with the previous Arctic Ocean silicate transports and budgets: the results of *Codispoti and Lowman*, 1973, referred hereinafter as CL73; *Codispoti and Owens*, 1975, referred hereinafter as CO75; *Jones and Coote*, 1980, referred hereinafter as JC80; and *Anderson et al*., 1983, referred hereinafter as AN83, which are summarized in Table 2. These studies are the first attempts to generate silicate transports and budgets for the Arctic Ocean; there are no equivalent studies for nitrate and phosphate. These four papers all evolved the structure of their Arctic Ocean silicate budget from the pioneering physical oceanographic work of *Coachman and Aagaard*, 1974 (referred to as CA74), which we describe first.

[27] CA74 (see their Table 6) divided their Arctic Ocean budget elements into inflows and outflows, and their volume transport values were all derived from 1960s publications (see CA74 for references). Their structure was recognizably sensible: inflows comprise the WSC, Bering Strait, the Barents Sea and rivers; outflows comprise the EGC, the Canadian Arctic Archipelago (CAA) throughflow, the Barents Sea again, and sea ice and meltwater. The WSC was vertically subdivided into Atlantic Water and the Arctic Bottom Water. CA74's Atlantic Water extended from the surface down to ~ 800 m, with its lower limit being defined by the 0°C isotherm; its salinity range was 34.0–35.2. Their

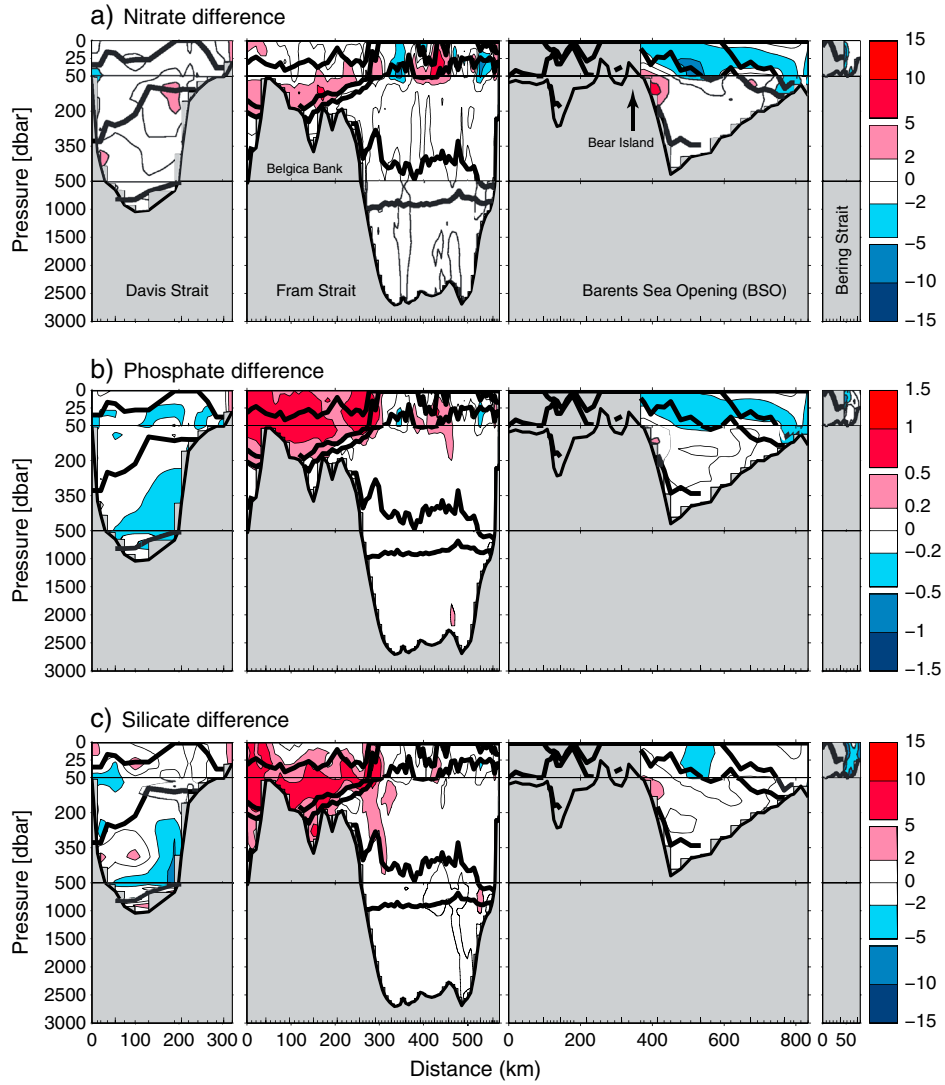

Figure 6. Nutrient concentration differences for secondary minus primary sections used in the assessment of nutrient transports uncertainty (details given in section 3.2). (a) Nitrate difference, (b) phosphate difference, and (c) silicate difference. Secondary data is formed by Davis Strait (September 2004), Fram Strait (September 1998), BSO (September 2003, data only available south of Bear Island), and Bering Strait (July 2005, when only the US sector was available). Regions for which secondary data were unavailable are grey-shaded. Primary data is formed by Davis Strait (September 2005), Fram Strait (September 2005), BSO (April/June 2002), and Bering Strait (August 2005). Color bars show nutrient concentrations in μmol L^{-1}. Note depth scale is expanded from 0–50, 50–500, and 500–3000 m.

Arctic Bottom Water lay beneath the Atlantic Water, with temperatures <0°C. CA74's EGC comprised the following: the Polar Water from the surface to ~150 m, with temperature between 0°C and the freezing point and salinity of 30–34; Atlantic Intermediate Water below it, down to ~800 m, with temperature >0°C and salinity of 34.88–35.0; and finally Deep Water, with temperature <0°C and salinity of 34.87–34.95.

[28] CA74's four volume budget case studies all contrived to make inflows equal outflows, at between 3.3 and 5.4 Sv each. Comparing these early budget estimates with the modern calculation of T2012, we can see that (balanced) inflows and outflows each totalling ~8 Sv is more realistic; furthermore, we can identify the most significant missing element of CA74's compilation: the Barents Sea. Only one of their four case studies includes a Barents Sea inflow at 1 Sv, and one other has no inflow but a small outflow at 0.05 Sv.

[29] The weakness of these early appreciations of the importance of the Barents Sea to Arctic Ocean budgets is perhaps surprising. The region has been visited by sealers and whalers for centuries, so that their records have been used to reconstruct multi-century histories of the ice edge [e.g., *Divine and Dick*, 2006; *Macias Fauria et al.*, 2009]. Indeed CA74 state that "numerous oceanographic data are available" for the Barents Sea. Direct velocity measurements of inflowing Atlantic water, made in 1978, were published in *Loeng et al.* [1997] and they show that an inflow of ~3 Sv is realistic. This will be discussed further below.

Table 2. Summary of Previous Silicate Transports and Budget Estimates for the Arctic Ocean[a]

Source	CL73			CO75			JC80			AN83			This study		
	V_T (Sv)	[Si] (μmol L^{-1})	Si_T (kmol s^{-1})	V_T (Sv)	[Si] (μmol L^{-1})	Si_T (kmol s^{-1})	V_T (Sv)	[Si] (μmol L^{-1})	Si_T (kmol s^{-1})	V_T (Sv)	[Si] (μmol L^{-1})	Si_T (kmol s^{-1})	V_T (Sv)	[Si] (μmol L^{-1})	Si_T (kmol s^{-1})
Inputs															
Atlantic Water and										0.48	5 ± 1[b]	2.4 ± 0.5			
Arctic Bottom Water	6	5	30	6	5	30	6	5	30	1.95	5 ± 1[b]	9.6 ± 2.0	3.8[c]	0 to 15[c]	22.8[c]
Bering Strait	1.5	35	52	1.5	35	52	1.5	35	52	1.35	23 ± 9[b]	31.1 ± 12.2	1.0[c]	2 to 40[c]	20.9[c]
River Discharge	0.1	150	15	0.1	125	12	0.1	125	12	0.11	125	13.2 ± 2.0	0.75[d]	52–317[d]	12.87[d]
BSO	np	np	np	np	np	np	np	np	np	np	np	np	3.8[c]	0 to 7[c]	13.2[c]
Others	np	np	np	np	np	np	np	np	np	np	np	np	0.2[c]	0 to 15[c]	4.3[c]
Sub-total	7.6		97	7.6		94	7.6		94	3.89		56.3 ± 16.7	5.55		56.6
Total													8.8		61.2
Outputs															
EGC	6.1	8	49	5.6	8	45	5.6	8	45	1.8	6 to 15[b]	18.4 ± 2.5	5.4[c]	0 to 10[c]	34.1[c]
CAA	1.5	10	15	2	16	32	2	21	42	2	11 to 25[b]	41.5 ± 2.0	3.0[e]	0.2 to 28[e]	49 ± 13[e]
Sea Ice	np	np	np	np	np	np	np	np	np	0.1	1	0.1 ± 0.1	0.05[f]	0.07[f]	3.5×10^{-3}
Davis Strait	np	np	np	np	np	np	np	np	np	np	np	np	3.1	0 to 40[c]	43
Others	np	np	np	np	np	np	np	np	np	np	np	np	0.4[c]	0 to 7[c]	0.0[c]
Sub-total	7.6		64	7.6		77	7.6		87	3.9		60.0 ± 4.7	8.45		83.1
Total													8.9		77.1
Inputs - Outputs															
Sub-totals	0		33	0		17	0		7	−0.01		−3.7	−2.95		−26.5
Totals													−0.1		−16

[a]CL73, *Codispoti and Lowman* [1973]; CO75, *Codispoti and Owens* [1975]; JC80, *Jones and Coote* [1980]; AN83, *Anderson et al.* [1983]; V_T, volume transport; [Si], average silicate concentration or concentration range; Si_T, silicate transport; np, not provided.

[b]*Anderson et al.* [1983] divided each gateway into various depth layers. Bering Strait has three layers, each of which was assigned with the same silicate concentration. The Atlantic Water was divided in inflows above 200 m and below 200 m (this is described in more detail in section 4.1.2). The range of silicate concentrations shown are those measured by *Jones and Coote* [1980] for the three main Sounds in the CAA.

[c]Values for the WSC, Bering Strait ("inputs"), and EGC ("outputs") taken from Table 1 here. Silicate concentration range is shown as per Figure 3.

[d]Data from *Holmes et al.* [2011]; river discharge converted from 2,348 $km^3\ yr^{-1}$; silicate concentration range for the major rivers delivering to the Arctic Ocean (PARTNERS, http://www.arcticgreatrivers.org/); Si-river discharge converted from 11.395×10^9 g yr^{-1}.

[e]CAA transports computed as described in section 4.1.3, by integrating constructed absolute velocity fields and silicate profiles (Figure 7).

[f]Ice transport as in T2012. Silicate concentration in multiyear ice from the Nansen Basin area north of Svalbard measured by *Tovar-Sánchez et al.* [2010].

4.1.2. Previous Silicate Transports

[30] The four previous Arctic Ocean silicate transport studies—CL73, CO75, JC80 and AN83—all based their budgets on CA74's volume transport structure, with similar inputs and outputs. Starting with CL73, silicate concentrations were "assigned" based on available data to the relevant water masses and were then combined with volume transports based mainly on CA74, which was at the time, still in press. For the Atlantic Water and the Arctic Bottom Water, a volume transport of 6 Sv was assumed to be reasonably representative of the range estimated until then. A silicate concentration of 5 μmol L^{-1} was assigned to both water masses. For Bering Strait, an estimated volume transport of 1.5 Sv and an average silicate concentration of 35 μmol L^{-1} were selected. For riverine inputs, the volume transport was taken from the compilation by CA74, and a silicate concentration of 150 μmol L^{-1} was assumed based on data available for the Mackenzie and Yukon rivers, and silicate concentrations measured at hydrographic stations close to the Lena River delta. For the EGC, a volume transport of 6 Sv was considered reasonable, in comparison with CA74's values of 2.0–4.1 Sv; however, it was taken to be 6.1 Sv in the final calculation of CL73 to achieve volume transport balance. A concentration of 8 μmol L^{-1} was assigned to the EGC. For the CAA, CL73 mentioned that the available information indicated the transport was 2 Sv, but they assigned a value of 1.5 Sv, again to balance the volume transport budget. A concentration of 10 μmol L^{-1} was assigned to this volume transport based on the data available for Kennedy Channel. Thus, their estimated total inputs and outputs were respectively 97 and 64 kmol-Si s^{-1}, resulting in an imbalance of 33 kmol s^{-1} and implying that the Arctic Ocean was a sink of silicate.

[31] CL73 pointed out that the lack of data in the CAA (in particular in Lancaster Sound) could result in the transport being underestimated there. Therefore, in a further study, CO75 revised the silicate transports and budget by including new data collected in Lancaster Sound, taking a silicate concentration of 20 μmol L^{-1}. A silicate concentration for Jones Sound, for which data was not available, was assumed to be intermediate between Lancaster Sound and Kennedy Channel; thus, a concentration of 15 μmol L^{-1} was used. This time, the CAA volume transport was taken as 2 Sv, and volume-weighted silicate concentrations for each channel were obtained based on the work by *Muench* [1970] who suggested that the relative volume transport contributions of each passage were 25% Kennedy Channel, 25% Jones Sound, and 50% Lancaster Sound, resulting in an average silicate concentration for the CAA of about 16 μmol L^{-1}. A lower river-derived silicate concentration was also assumed, at 125 instead of 150 μmol L^{-1}. Again, though it was not explained, it seems the volume transport for the EGC was adjusted, this time to 5.6 Sv, in order to accommodate the new volume transport through the CAA. The budget resulted in a smaller (still positive) imbalance of 17 kmol s^{-1} by slightly reducing inputs to 94 kmol-Si s^{-1} but significantly increasing the outputs to 77 kmol-Si s^{-1}. The conclusion that the Arctic Ocean was a sink for silicate still held.

[32] JC80 then used more data from a far more thorough survey of the CAA, which indicated a higher silicate content there: 25 μmol L^{-1} in Lancaster Sound, 22 μmol L^{-1} in Fram Sound (the mouth of Jones Sound), and 11 μmol L^{-1} in Smith Sound, the southern end of Kennedy Channel. The resulting average silicate concentration was thus 21 μmol L^{-1}, as opposed to the 10 and 16 μmol L^{-1} previously used. JC80 updated the budget again by including these new silicate data, resulting in 94 kmol-Si s^{-1} inputs and 87 kmol-Si s^{-1} outputs, and thus an even smaller imbalance at 7 kmol s^{-1}. These authors concluded that inputs and outputs were in good agreement given uncertainties related to volume transports, thereby not supporting the case of the Arctic being a silicate sink. Since the studies by CL73, CO75, and JC80 used the same configuration of water masses and Arctic gateways, it seemed that improving the data coverage and consequently average silicate concentrations helped to constrain the original budget (Table 2).

[33] AN83 calculated a more detailed budget. Arctic river discharges were compiled from (new at the time) published data, which included the Siberian rivers, but the average silicate concentration used was that by CO75. For the CAA, AN83 based their study on CO75 and JC80 but assigned an uncertainty of ± 1 μmol L^{-1} to each of the sounds' average silicate concentrations. For Bering Strait and Fram Strait, AN83 based their calculations on various studies then available (see AN83 and references therein). Bering Strait was structured in three 15 m layers, each with a 0.45 Sv volume transport, a silicate concentration of 23 μmol L^{-1}, and an assigned uncertainty of ± 9 μmol L^{-1}. The EGC was structured in 50 m layers down to 200 m, with average silicate concentrations between 6 and 15 μmol L^{-1} and associated uncertainties being ± 1 or ± 2 μmol L^{-1}. For the inputs through Fram Strait (i.e., the WSC), the upper 200 m were structured in 50 m layers, with volume transports between 0.10 and 0.14 Sv from 0 m down to 200 m. It is important to note that the volume transport from 200 down to 2000 m was adjusted arbitrarily to balance the volume transport budget. Average silicate concentrations of 5 ± 1 μmol L^{-1} were assumed for all layers. In addition to differences in water mass structure and associated average silicate concentrations, relative to previous estimates, volume transports across Fram Strait (both input and output) are notably most different, being ~ 3 times lower in AN83 compared with the previous studies. The resulting total transports of 56.3 ± 16.7 kmol-Si s^{-1} (inputs) and 60 ± 4.7 kmol-Si s^{-1} (outputs) are thus comparatively lower. These result in an imbalance of -3.7 kmol-Si s^{-1}, so AN83 also concluded the silicate budget to be balanced. Note that their uncertainties in total transports result from adding the uncertainties of estimated individual transports (Table 2). Like the three preceding studies, the AN83 budget also lacks transports through the BSO, and consideration of the EGC only down to 200 m renders the outflow there incomplete.

4.1.3. Canadian Arctic Archipelago Transports

[34] Before comparing our silicate transports with the earlier studies (section 4.1.4 below), we first digress on the question of CAA transports, for two reasons: to assess an aspect of the previous method of calculation of Archipelago transports, and to be able to compare our Davis Strait transports with preceding CAA transport estimates. We discuss these two issues in order.

[35] We address first a source of bias in previous silicate transport calculations. It is generally true that the nutrient concentrations in all the circum-Arctic gateways increase with depth, with the exception of the shallow Bering Strait. At the same time, velocities are generally a maximum at the surface

and decrease with depth. Now consider any strait and define means of velocity v, nutrient concentration n (overbar), and anomalies from the means (prime), such that $v' = v - \bar{v}$ (and similarly for n'), so

$$\bar{v} = \int v dA/A \tag{2}$$

and

$$\int v' dA = 0 \tag{3}$$

and similarly for n, where dA is a cross-section area element and A is the total cross-section area (c.f., T2012). Total nutrient transports T_n will then be given by

$$\begin{aligned} T_n &= \int vndA \\ &= \bar{v}A\bar{n} + \int v'n'dA \end{aligned} \tag{4}$$

[36] where the first term on the right hand side is just the total volume transport multiplied by the mean nutrient transport, and the second term describes the contribution to the net nutrient transport when correlations between velocity and nutrient concentration anomalies are non-zero. Not only is this term non-zero around the Arctic boundary but also is generally negative, because nutrient concentrations increase with depth while velocities decrease. Therefore, any nutrient transport calculation that simply multiplies the mean volume transport by the mean nutrient concentration will always be biased high, and we will assess the size of the bias below.

[37] Now, we address the issue of CAA volume and nutrient transports. We have no velocity or silicate observations in the CAA for summer 2005, so we proceed to estimate silicate transports through the CAA using available information. The approach is to "back out" CAA transports using Davis Strait transports as a starting point. The differences between the net CAA throughflow and the net Davis Strait export are as follows: (1) Fury and Hecla Strait, already shown to be negligible in T2012, and (2) any additional volume flux inputs to Baffin Bay. Baffin Bay inputs are essentially small freshwater terms: CAA sea ice export, 6 ± 1 mSv [*Agnew et al*., 2008; *Kwok*, 2006]; Greenland ice sheet melt, 7 ± 1 mSv [*Mernild et al*., 2009]; the excess of precipitation over evaporation, 7 ± 4 mSv [*Jensen and Rasch*, 2008]; and Baffin Island runoff, 3 ± 1 mSv [*Canadian Climate and Data Information Archive*: http://climate.weatheroffice.gc.ca/]. The sum of these terms is very small and also negligible, so our approach is valid in terms of mass conservation.

[38] The Davis Strait sill depth is 650 m [*Rudels*, 2011], and the volume flux through Davis Strait above sill depth is 3.0 Sv. We next need to decide how to partition this total volume flux between the three CAA straits to the north: Lancaster and Jones Sounds, and Nares Strait. We first consider silicate measurements, which will guide our approach. There are few available silicate measurements in the CAA (Figure 7). We find one silicate profile in the middle of Lancaster Sound (July–August 2005) [Beaufort Gyre Project at http://www.whoi.edu/beaufortgyre; *McLaughlin et al*., 2010]. Five profiles along Smith Sound, at the southern end of Nares Strait, were measured by the Canadian Archipelago Through-flow Study project during July–August 2003 (http://www.udel.edu/CAT). No silicate data is available in Jones Sound. Both Lancaster Sound and Nares Strait show typical silicate profiles: low at the surface, high at the bottom, with mean silicate concentrations of 21.1 and 11.3 μmol L^{-1}, respectively, similar to JC80's values of 25 and 22 μmol L^{-1} in Lancaster and Jones Sounds, respectively, and 11 μmol L^{-1} in Nares Strait.

[39] Published measurements of volume transports through these three straits (as compiled by *Curry et al*. [2011]) are 0.7 Sv for Lancaster Sound [*Prinsenberg et al*., 2009], 0.3 Sv for Jones Sound [*Melling et al*., 2008], and 0.72 Sv for Nares Strait [*Munchow and Melling*, 2008; *Rabe et al*., 2010]. Given that, for Jones Sound, (1) its volume flux is small, (2) its silicate concentration is reportedly similar to the Lancaster Sound concentration, and (3) there are no modern silicate measurements available, we choose to aggregate the volume fluxes for Jones and Lancaster Sound and ascribe the same silicate concentration to them. To translate our Davis Strait volume northward, we preserve the ratio of the volume fluxes ascribed to Lancaster Sound (including Jones Sound) and Nares Strait, 1.0:0.7 Sv, or ∼ 2:1. Finally, we wish to include realistic vertical velocity shear. Velocity measurements in Lancaster Sound and Nares Strait are published for 1998–2007 [*Prinsenberg and Hamilton*, 2005; *Melling et al*., 2008] and 2003–2006 [*Rabe et al*., 2010], respectively. Velocity sections show typical profiles, high at the surface and low at the bottom. Taking the average vertical velocity shears for the two straits, the bottom velocities are then adjusted to give the required strait transports.

[40] Total silicate transports are estimated by integrating the constructed absolute velocity fields and silicate data (as described above) across the two straits. The silicate transport uncertainty is estimated by (1) changing the ratio of volume transports between Lancaster Sound and Nares Strait and (2) varying the silicate concentration in both straits by ±30%. The ratios of volume transports of Lancaster Sound and Nares Straits are prescribed as high and low alternates of 3:1 and 11:9, around the standard setting of 2:1. The silicate transport uncertainty is then calculated from nine sensitivity runs, obtained by permutations of the three sets of velocity fields and the three sets of nutrient sections. The resulting silicate transport through the CAA in summer 2005 is -49.0 ± 13.0 kmol-Si s^{-1} (-25.8 ± 6.7 kmol-nitrate s^{-1} and -3.6 ± 0.9 kmol-phosphate s^{-1}). The silicate transport obtained as the sum of the products of mean silicate concentrations and mean volume transports in Lancaster Sound and Nares Strait is instead 53.4 kmol s^{-1}, biased high by ∼ 10%.

4.1.4. Comparison with New Silicate Transports and Budget

[41] In Table 2, we present our results structured for comparability with the studies described in section 4.1.2. For inputs, we select transports for Bering Strait and the WSC from Table 1 and we include the most recent available data on nutrient river loads from *Holmes et al*. [2011]. For outputs, we select transports for the EGC from Table 1, while for transports via the CAA, we use the results of section 4.1.3.

[42] Starting with riverine transports (since these are the non-oceanic component), silicate river loads are surprisingly similar between the estimates by CO75, JC80, and AN83,

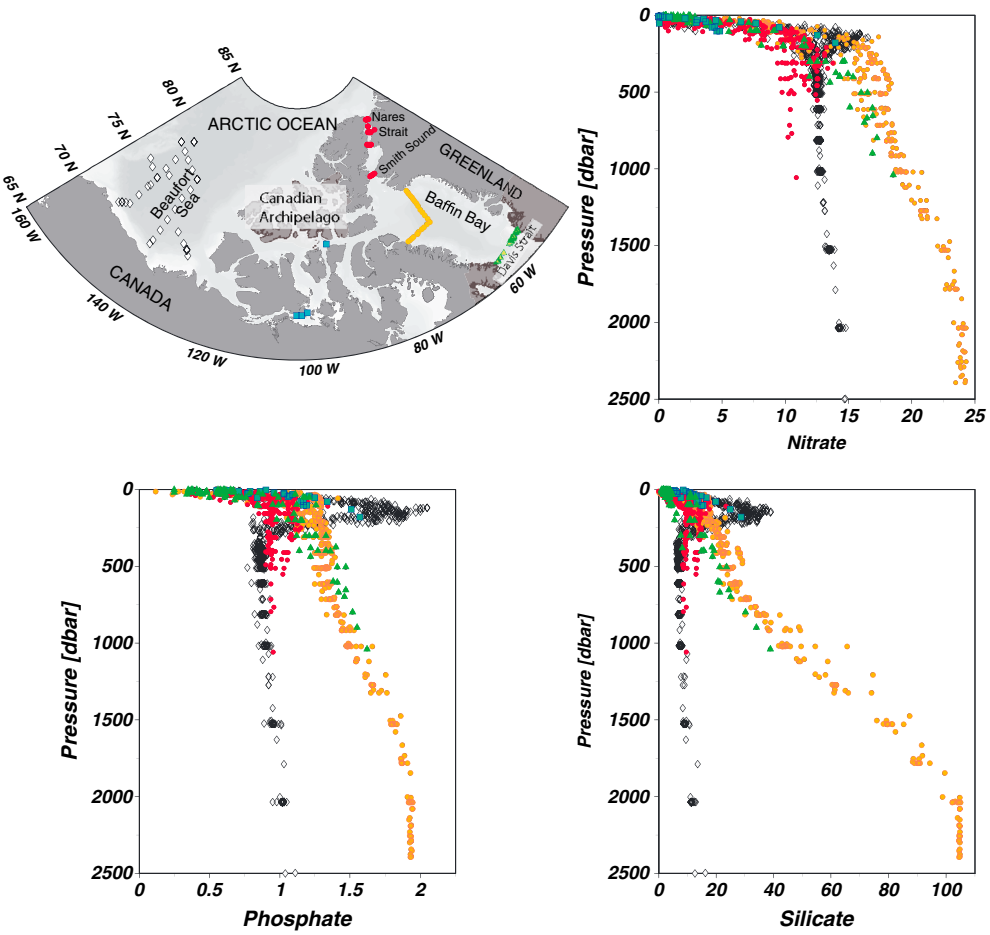

Figure 7. Nitrate, phosphate, and silicate profiles (μmol L^{-1}) from the Arctic interior (Beaufort Gyre sector, ◇), Canadian Archipelago (◆), Nares Strait and Smith Sound (●), Baffin Bay (●), and Davis Strait (▲). Beaufort Gyre and Canadian Archipelago data are from the Beaufort Gyre Project at http://www.whoi.edu/beaufortgyre (July–August 2005). Nares Strait, Smith Sound, and Baffin Bay data are from the Canadian Archipelago Throughflow Study Project (CATS) at http://www.udel.edu/CATS (July–August 2003). Davis Strait data are as described in section 2.2.

and those measured by *Holmes et al*. [2011] all are within a range of 12–15 kmol-Si s^{-1} (Table 2).

[43] For the WSC (or equivalent), the volume transports used in the first three studies roughly doubled those of AN83 and the present study. The average concentration of 5 μmol L^{-1} used previously does not capture the vertical silicate gradient of about 0 to 15 μmol L^{-1} (Figure 3c). Our silicate transport computation thus lies between that of AN83 and those of CL73, CO75, and JC80, within about 10 kmol-Si s^{-1}.

[44] The volume transport through Bering Strait in the previous studies is higher (by 0.35–0.5 Sv) than ours, and the average silicate concentrations (23–35 μmol L^{-1}) may overestimate the horizontal gradient ($\sim$ 2 to 40 μmol L^{-1}) across Bering Strait. The resulting transports in previous studies are 10 to 30 kmol-Si s^{-1} larger than our computation.

[45] Other than the volume transport used by AN83 for the EGC (which is the lowest of all by a factor of >3, given it was only considered down to 200 m depth), volume transports used by previous studies are comparable to ours within 0.7 Sv. Despite the fact that the silicate concentration range used by AN83 contains higher concentrations relative to the averages used in previous studies and relative to the vertical gradient used in our computations, their silicate transport for the EGC is lower than ours by 15 kmol-Si s^{-1}, and by $\sim$30 kmol-Si s^{-1} relative to previous studies..

[46] For the CAA, AN83 based their silicate transport estimate on the two previous studies and are therefore similar to the estimate by JC80. Volume transports are comparable among all studies within 0.5 Sv. Our silicate transport computations for the CAA as described in section 4.1.3 are comparable to those obtained by JC80 and AN83, but higher that those by CL73 and CO75 by 34 and 17 kmol-Si s^{-1}, respectively. Nonetheless, our calculations indicate that estimating nutrient transports simply by multiplying the mean volume transport by the mean silicate concentration biases the result high. Our silicate transport via Davis Strait is also similar to the CAA transports obtained by JC80 and AN83. The main difference between transports across the CAA and those computed at Davis Strait is the apparent transfer of nutrients from near-surface to deeper waters, and we proceed to inspect this feature more closely.

[47] In Figure 7, we show the vertical profiles of the three nutrients from three groups of locations: first, the Beaufort Sea, representing upstream nutrient distributions; second, the CAA (data from Queen Maud Gulf, Barrow Strait, and Nares Strait); and third, Baffin Bay. The consistent picture that emerges is the high concentrations of nutrients at depths around 100–200 m in the Beaufort Sea with much lower concentrations above and below, transforming into Baffin Bay nutrient concentrations that increase nearly monotonically with depth, from low at the surface to deep values as high as, or considerably higher than, the Beaufort Sea near-surface maxima. Concentrations across Davis Strait are comparable to those in the Baffin Bay at similar depths. This is consistent with the proposed mechanism whereby nutrients are transferred from near-surface to deep waters via sinking of biogenic particles [*Michel et al*., 2002; *Tremblay et al*., 2002a, 2002b].

[48] Finally, in terms of total inputs and total outputs as presented in Table 2, our total inputs are similar to those by AN83, and our output estimates are similar to those by JC80. In general, similarities between our computations and those of the previous studies seem to be partly due to ingenious choices made by the previous authors on the basis of little data, and partly due to luck. In those earlier studies, volume transport balance was achieved via arbitrary adjustments; silicate transports did not always take into account vertical and horizontal velocity and silicate gradients; and most importantly, they lacked an appreciation of the importance of the BSO, which contributes 4 Sv and 17.5 kmol-Si s^{-1} to the inflow. When the missing information is incorporated, volume transport is conserved and the resulting total silicate outflow is larger than the total inflow. This eventually results in an imbalance in the ocean silicate budget of ca. −16 kmol-Si s^{-1}.

4.1.5. Comparison with Previous Indirect Estimates

[49] Based on biogeochemical budgets and nutrient consumption ratios, *Macdonald et al*. [2010] inferred (1) the amount of nutrients that are required to sustain their estimates of export production over the Arctic Shelves and (2) the potential imports of nutrients from the Pacific and Atlantic Oceans (both summarized here in Table 3). They pointed out that oceanic nutrient imports together with upwelling and shelf exchange may be enough to support their estimated rates of export production over the Chukchi and Barents Sea shelves. How do our computations compare with their oceanic nutrient import estimates, and how much of the estimated export could these thus sustain? Our computed silicate transport of ∼21 kmol s^{-1} through Bering Strait is similar to that estimated by *Macdonald et al*. [2010], of ∼22 kmol s^{-1}, and can thus support ∼80% of the estimated export (26.3 kmol-Si s^{-1}). For nitrate and phosphate transports, our computations are lower by 7.5 kmol-N s^{-1} and 0.7 kmol-P s^{-1} than the estimated Pacific inflow of 16.5 kmol-N s^{-1} and 2 kmol-P s^{-1}. Only phosphate seems to be supplied in excess, by 0.5 kmol s^{-1}, of the estimated requirement of 0.76 kmol s^{-1}. For the BSO, our computations of net nitrate and phosphate transports are larger by 7.6 kmol-N s^{-1} and 0.6 kmol-P s^{-1} than the estimated imports of 26 kmol-N s^{-1} and 1.8 kmol-P s^{-1} and are in excess by 3 kmol-N s^{-1} and 0.5 kmol-P s^{-1} of the estimated 30 kmol-N s^{-1} and ∼1.9 kmol-P s^{-1} required to sustain the *Macdonald et al*. [2010] export production in the Barents Sea. In contrast, the 13 kmol s^{-1} supply of silicate would only provide ∼20% of the required amount (64 kmol s^{-1}). The oceanic supply of nutrients is thus relevant as it fuels an important proportion of primary and export production over these shelves. Although, as suggested by the biochemical budgeting study by *Macdonald et al*. [2010], most of the nutrients taken up are eventually regenerated back into the water column and are therefore transported elsewhere and possibly exported from the Arctic Ocean.

Table 3. Summary of Inferred Nutrient Requirements to Sustain Estimates of New Production Over the Chukchi Sea and Barents Sea, and Estimated Pacific and Atlantic Nutrient Imports by *Macdonald et al*. [2010][a]

	Nitrogen	Phosphorus	Silicate
Chukchi Sea Requirement	12.4	0.76	26.3
Pacific Inflow	16.5	2.06	21.87
Barents Sea Requirement	30.1	1.87	64.05
Atlantic Inflow	26	1.80	9.98

[a]Values converted to kmol s^{-1} from Table 6.2.4 in *Macdonald et al*. [2010]. Note that these authors refer to nitrogen and phosphorus, rather than the chemical species nitrate and phosphate.

4.2. Additional Sources of Inorganic Nutrients

[50] As explained earlier, our main nutrient transports and budget computations focus only on oceanic fluxes of dissolved inorganic nutrients. Our computations suggest silicate and phosphate are exported from the Arctic Ocean, so in this section, we explore alternative nutrient sources that may offset these oceanic imbalances. Though oceanic nitrate transports are found to be balanced, denitrification in the Arctic Ocean is estimated to remove between ∼ 14–66 kmol-nitrogen s^{-1} (6–29 Tg-N yr^{-1}; *Chang and Devol* [2009]), implying that additional sources of nitrogen must exist too.

[51] After oceanic transports, rivers are likely to be the largest external source of nutrients to the upper layers of the Arctic Ocean. On average, fluvial nutrient loads deliver the equivalent of ∼1 kmol s^{-1} of dissolved inorganic nitrogen (of which ∼0.8 kmol s^{-1} is delivered in the form of nitrate), 0.07 kmol s^{-1} of total dissolved phosphorus (including both inorganic and organic fractions), and 12.9 kmol s^{-1} of silicate [*Holmes et al*., 2011]. River nutrient inputs could thus account for a substantial proportion (∼82%) of the silicate imbalance, but only a small proportion (∼7%) of the phosphate imbalance. The fluvial input of dissolved inorganic nitrogen would only account for 1.5%–7% of the nitrogen loss via denitrification.

[52] Sources such as glacial biogeochemical weathering and fine sediment transports by glaciers perhaps supply small amounts of nutrients locally [e.g., *DeMaster*, 1981; *Hodson et al*., 1998; *Hodson et al*., 2005; *Wadham et al*., 2010]. Atmospheric deposition of nutrients is thought to be minor in the Arctic Ocean [e.g., *Macdonald et al*., 2010; *Kanakidou et al*., 2012], and nitrogen fixation rates in the Beaufort Sea region (0.0065 mmol-N m^{-2} day^{-1}) would only account for ∼0.7% the nitrogen loss through denitrification (1 mmol-N m^{-2} d^{-1}) [*Blais et al*., 2012].

[53] External inputs, oceanic and riverine, of dissolved organic matter (DOM) to the Arctic Ocean may provide additional inorganic nutrients following remineralization

and UV oxidation processes. Available evidence shows that while the N:P ratio of DOM is highly variable, it is overall high [e.g., *Simpson et al*., 2008; *Torres-Valdes et al*., 2009; *Holmes et al*., 2011]. Hence, it is likely that the contribution of dissolved organic nitrogen (DON) to the dissolved inorganic nitrogen pool is higher than the contribution of the dissolved organic phosphorus (DOP) to the dissolved inorganic phosphorus pool. The ratio of DON to the total dissolved phosphorus annual river loads in the Arctic is ~25 [*Holmes et al*., 2011]. In the Beaufort Sea region of the Arctic Ocean, the DON:DOP ratio has been observed to be as high as 200 (mol/mol) [*Simpson et al*., 2008]; elsewhere in the ocean, DON:DOP ratios are on average 56 ± 36 [*Torres-Valdes et al*., 2009]. Besides, DOP is also likely to be utilized faster than DON, given that it is mostly labile [e.g., *Clark et al*., 1998; *Karl and Björkman*, 2002; *Björkman and Karl*, 2003; *Duhamel et al*., 2010].

[54] As mentioned above, river inputs of DOP are low, but the supply of DON is almost twice the inputs of dissolved inorganic nitrogen at ≈1.92 kmol-N s^{-1} [*Holmes et al*., 2011]. A model study by *Tank et al*. [2011] suggests that 0.4–0.6 and 0.06–0.1 kmol s^{-1} of the DON river loads are respectively regenerated over the shelves and open ocean waters of the Arctic. These, combined with the riverine supply of total dissolved inorganic nitrogen, would yield 1.46 to 1.7 kmol-N s^{-1} that could account for ~2%–12% of the nitrogen removal via denitrification.

[55] Elsewhere in the ocean, dissolved organic nutrients are known to dominate nutrient pools in the upper layers [e.g., *Mahaffey et al*., 2004; *Raimbault et al*., 2008; *Torres-Valdes et al*., 2009], where the interplay of recycling and transport processes help sustain a proportion of primary production downstream [e.g., *Roussenov et al*., 2006; *Torres-Valdes et al*., 2009]. Currently, estimates of oceanic transports of dissolved organic nutrients across the Arctic Ocean boundaries are not available. Measurements have been carried out in the southeastern Beaufort Sea by *Simpson et al*. [2008], where DON concentrations average to 4.6 ± 3.7 μmol L^{-1} (range 0.2–35.8 μmol L^{-1}) and DOP averages to 0.65 ± 0.38 μmol L^{-1} (ranging from the limit of detection to 2.3 μmol L^{-1}). There, a DOP maximum (0.76 ± 0.27 μmol L^{-1}) was found to be associated with waters of 33.1 salinity. By examining the relationship between DOP and the tracer N^* (useful for tracing waters of Pacific origin) at salinities 30 to 33.1, it was found that waters derived from the Bering Sea were more enriched in DOP than the other water masses in that region [*Simpson et al*., 2008]. This suggests that waters flowing into the Arctic Ocean via Bering Strait could provide a source of dissolved organic nutrients (at least in the case of DOP). We are not aware of any DON and DOP measurements from the Atlantic sector of the Nordic Seas (i.e., the Norwegian Sea). A simple calculation provides a rough estimate of the average oceanic DON and DOP concentrations that would be required to offset the phosphate imbalance and the nitrogen loss. Since the volume outflow and the volume inflow are similar at about 8.8 Sv and given the phosphate export of −1 kmol s^{-1}, we have that 1 kmol s^{-1}/8.8 × 10^6 m^3 s^{-1} ≈ 1 × 10^9 μmol/8.8 × 10^9 L, yielding an average DOP concentration of ~ 0.11 μmol L^{-1}. This can be repeated with the estimated range of nitrogen removal through denitrification, which yields an average DON concentration of 1.5–7.5 μmol L^{-1}. However, observations are required to test the hypothesis that oceanic transports of DON and DOP can account for the phosphate imbalance and the nitrogen loss via denitrification.

[56] In summary, silicate riverine inputs into the Arctic Ocean may account for the silicate imbalance. This implies that further changes in the hydrological cycle within the Arctic realm would affect the transfer of nutrients from the Arctic Ocean to the North Atlantic. Available information suggests that external sources of inorganic nutrients cannot account either for the phosphate imbalance found or for the losses of nitrogen through denitrification. DON riverine inputs could provide a proportion of the nitrogen loss, but cannot provide enough DOP. This leaves oceanic transports of dissolved organic nutrients as a potential additional source of nutrients to offset losses and imbalances in the Arctic Ocean nutrient budget.

4.3. Relevance and Potential Fate of Nutrient Exports

[57] Following the study by *Yamamoto-Kawai et al*. [2006], here we wish to gain further insight into the transfer of excess phosphate to the North Atlantic by computing P^* (P^* = phosphate − nitrate / 16) [*Deutsch et al*., 2007], thus taking advantage of the full depth sections around the Arctic Ocean boundary. Figure 8 shows the distribution and cumulative transports of P^* across the Arctic Ocean gateways (also given in Table 1). Consistent with the N:P ratio characteristic of Atlantic Waters [e.g., *Jones et al*., 1998], P^* concentrations are lowest (< 0.2 μmol L^{-1}) across most of Fram Strait and the BSO (Figure 8a). The highest values (0.6–1.0 μmol L^{-1}), which are consistent with Pacific-derived waters [e.g., *Jones et al*., 1998], occur across Bering Strait and in the upper 100 m on the western side of Davis Strait. Concentrations between 0.4–0.6 μmol L^{-1} can be observed in Davis Strait down to the bottom, in agreement with Baffin Bay bottom waters also having a low N:P ratio [*Jones et al*., 1984]. The net outflow via Fram Strait is smaller than that via Davis Strait by a factor of 6. Again, the P^* outflow via Davis Strait is larger than the input via Bering Strait, suggesting that excess phosphate may not only be provided by Pacific-derived phosphate. The resulting net P^* transport is −1.1 ± 0.3 kmol s^{-1} (net ± 1 standard error), which is almost twice as large as the 0.63 kmol s^{-1} (2 × 10^{10} mol yr^{-1}) estimated by *Yamamoto-Kawai et al*. [2006] by multiplying the average volume transport through Bering Strait by the concentration at the intercept of the slope of a dissolved inorganic nitrogen versus dissolved inorganic phosphorus plot.

[58] Recently, *Palter et al*. [2011] calculated the southwards physical supply of P^* (≃0.63 kmol s^{-1}) to the northwest boundary of the North Atlantic Subtropical Gyre. Their calculations, which include Ekman advection and along-isopycnal mixing, suggest that transports of P^* could potentially support ≃9.5 kmol s^{-1} of the biological nitrogen fixation along a section of the Gulf Stream as it separates from the eastern seaboard of North America. Of their calculated transport, Ekman advection transfers ≃0.47 ± 0.25 kmol-P^* s^{-1} from colder waters north of the gyre's northwest boundary southwards across the Gulf Stream (between its separation from the coast off Cape Hatteras and 45°W). The southward transport (i.e., via Davis Strait and Fram Strait) of P^* from the Arctic Ocean computed here could provide more than

four times the excess phosphate transfer across the Gulf Stream calculated by *Palter et al*. [2011].

[59] Given that nutrient transports from the Arctic Ocean are associated with different density surfaces, we wished to explore their potential spread within the North Atlantic. Waters of Pacific origin have been traced by *Jones et al*. [2003] from the CAA down to the Tail of the Banks, and transport and freshwater have been traced in the western North Atlantic from the tip of Greenland and Davis Strait to the east coast of North America by *Loder et al*. [1998]. Both studies show the relevance of Davis Strait outflows to the eastern North American shelf-slope system. Thus, in order to investigate possible transport pathways, we explored nutrient distributions along the isopycnal surfaces associated with largest exports from the Arctic Ocean using HydroBase annual climatologies (http://www.whoi.edu/science/PO/hydrobase/index.html). Figure 9a shows the distribution of isopycnal surfaces $\sigma_0 = 26.0$, 27.1, and 27.5 kg m^{-3} and associated depths over the North Atlantic Ocean, which correspond to the boundaries between AW, UAW, SubW, and SW (as per Figure 2a and as pointed out in Figure 8a). Figures 9b–9d show the distribution of silicate, phosphate, and nitrate along the isopycnal surfaces above.

[60] The isopycnal $\sigma_0 = 26.0$ kg m^{-3} does not outcrop north of ~50°. Denser layers suggest waters outflowing through Davis Strait are confined within the subpolar gyre. The pathway that nutrient transports are likely to follow is better illustrated by the distribution of silicate; a band of high concentrations ($\gtrsim$12 μmol L^{-1}) can be observed along the Labrador shelf break along isopycnal $\sigma_0 = 27.5$ kg m^{-1}, extending southward down to the southwest boundary of the subpolar gyre (Figure 9). Despite the fact that these concentrations are low relative to those observed at Davis Strait due to the smoothing in the climatologies, this pathway is consistent with the distribution of waters of Pacific origin, which flow close to the surface (upper 200 m) along the Labrador Current [*Jones et al*., 2003]. Additionally, it also suggests denser waters outflowing Davis Strait likely follow this same route. However, nutrient transports are expected to decrease as the southward flowing waters interact with adjacent waters [e.g., *Loder et al*., 1998; *Cuny et al*., 2005; *Azetsu-Scott and Yeats*, 2007]. The outflow via Fram Strait, which is probably partly of Pacific origin given the relatively high P^*, most likely dilutes as it flows southward. Pacific waters traced along the eastern side of Greenland fade at about 60°N [*Jones et al*., 2003]. It is also possible that waters of Pacific origin in this region may be only occasionally present, given that their outflow through Fram Strait is highly variable. Shifts in the Arctic Ocean surface circulation may confine them within the Beaufort gyre and/or force them to flow via the CAA [*McLaughlin et al*., 1996; *Falck et al*., 2005].

[61] While the analysis of climatologies is only illustrative, the emerging picture is consistent with nutrient-rich waters exported from the Arctic Ocean via Davis Strait being the major up-stream source of nutrients for the North American eastern shelf complex, in particular for the Newfoundland and Labrador shelves [*Loder et al*., 1998]. Furthermore, this outflow may supply nutrients directly to the southwest boundary of the subpolar gyre, where waters then may

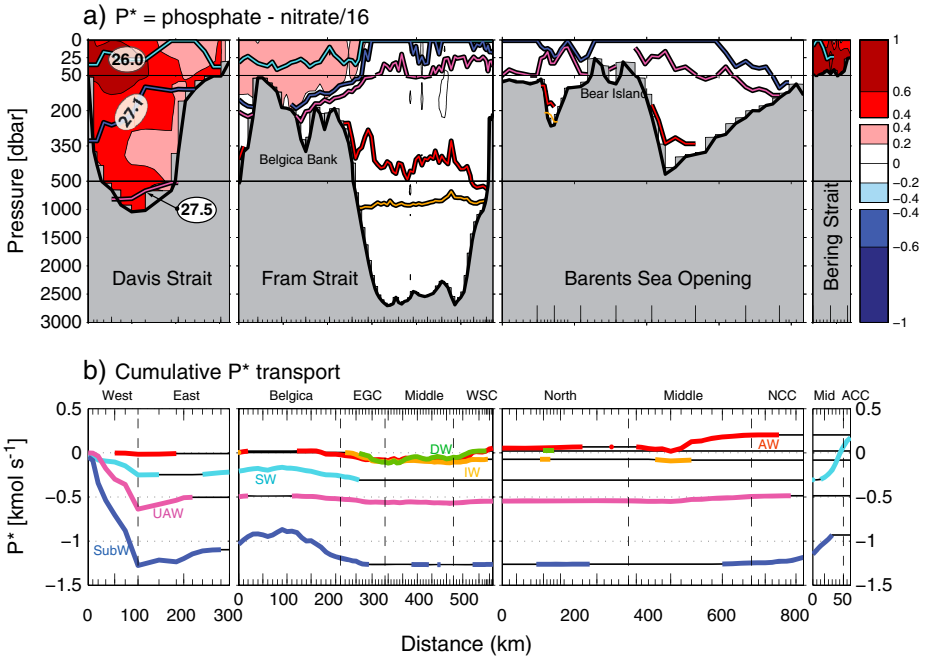

Figure 8. (a) P^* section across the main Arctic Ocean gateways and (b) cumulative P^* transport. $P^* = phosphate - nitrate/16$ [*Deutsch et al*., 2007]. Isopycnal surfaces $\sigma_0 = 26.0$, 27.1 and 27.5 kg m^{-3} in Figure 8a are shown for reference (see text). These isopycnal surfaces correspond to the boundaries between Atlantic Water, Upper Atlantic Water, Subsurface Water, and Surface Water, and are color-coded as in Figure 8b. Color bar shows concentration in µmol L^{-1}. Cumulative P^* transport is given in kmol s^{-1}. Components per section are shown for reference as per Table 1.

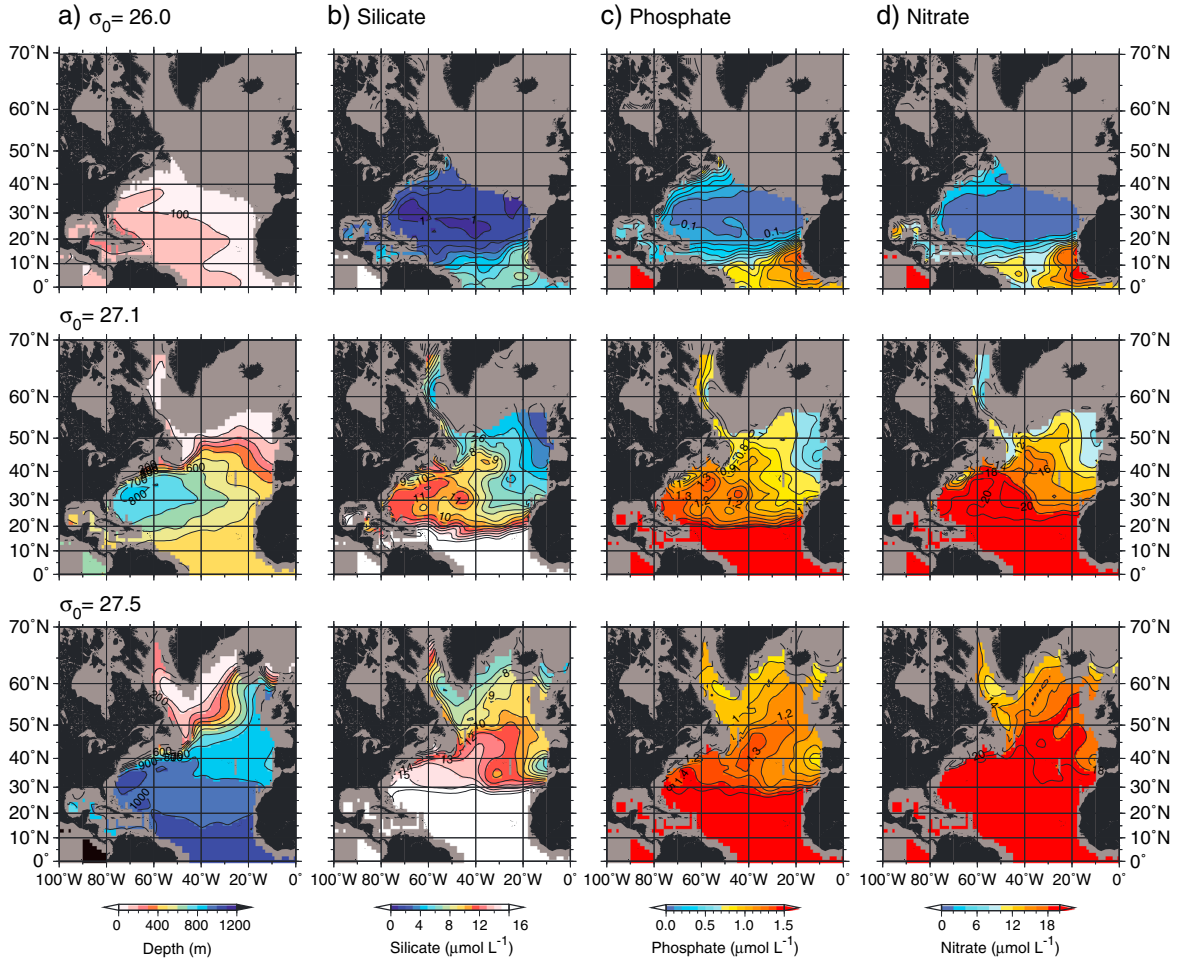

Figure 9. Property distributions in the North Atlantic showing: (a) isopycnal surfaces $\sigma_0 = 26.0$, 27.1 and 27.5 kg m^{-3} and depth at which these occur; and (b) silicate, (c) phosphate, and (d) nitrate along isopycnal surfaces shown in Figure 9a. Data from HydroBase annual climatologies (http://www.whoi.edu/science/PO/hydrobase/index.html).

further interact with the Gulf Stream and the sub-tropical gyre. Nutrient exports from the Arctic Ocean appear to be significant contributors to the North Atlantic Ocean nutrient budgets, accounting for $\sim$ 12% of the -130 ± 50 kmol s^{-1} net silicate transport and $\sim$ 90% of the -1.1 ± 2.5 kmol s^{-1} net phosphate transport estimated at 47°N by *Ganachaud and Wunsch* [2002]. Since the oceanic nitrate budget of the Arctic appears balanced, the transport of -10 ± 35 kmol-nitrate s^{-1} computed by *Ganachaud and Wunsch* [2002] at 47°N implies that an additional source of nitrate may exist in between.

5. Conclusions

[62] We provide physically based mass-balanced transport estimates of dissolved inorganic nutrients—nitrate, phosphate, and silicate—for the Arctic Ocean in summer 2005, which represent baseline calculations against which other and future estimates can be compared. We have quantified nutrient transports across Davis Strait, Fram Strait, the BSO, and Bering Strait (Figures 4 and 5), which are consistent with current knowledge of water mass circulation patterns across these gateways. We show that the major exports of all nutrients to the North Atlantic occur via Davis Strait. Nutrient transports associated with the EGC and with the WSC are almost balanced across Fram Strait. The largest imports of nitrate and phosphate to the Arctic Ocean occur via the BSO, and the largest import of silicate to the Arctic occurs via Bering Strait. We find that significant transport imbalances exist for silicate and phosphate, which result in the net export of these two nutrients (-15.7 ± 3.2 kmol-silicate s^{-1} and -1.0 ± 0.3 kmol-phosphate s^{-1}) from the Arctic Ocean to the North Atlantic. In contrast, the oceanic nitrate budget is balanced within the uncertainty (1.0 ± 1.6 kmol s^{-1}). The phosphate and silicate imbalances, together with current estimates of denitrification in the Arctic, prompted us to explore alternative sources of nutrients that may offset imbalances and losses. For silicate, most of the imbalance (82%) can be provided by riverine inputs. However, for phosphate, these are not enough (only $\sim$7%). For nitrogen, available information suggests that the combination of river inputs of dissolved inorganic and dissolved organic nitrogen and nitrogen fixation could supply $\sim$13% of the nitrogen loss via denitrification. Sources other than the ocean and rivers seem to be minor. Oceanic inputs of dissolved organic nutrients are hypothesized to account for the phosphate

imbalance and the losses of nitrogen through denitrification. We have also computed the net transport of excess phosphate at -1.1 ± 0.3 kmol-$P^{\star}$ s^{-1}, which is larger than previously estimated. Silicate and phosphate exports from the Arctic Ocean supply an important fraction of the North Atlantic nutrient budget, but in the case of nitrogen, calculations imply that an additional source of nitrate may exist between the Arctic and the North Atlantic across 47°N.

[63] **Acknowledgments.** This study was funded by the UK Natural Environment Research Council as a contribution to the Arctic IPY project Arctic Synoptic Basin-wide Oceanography (ASBO). Data obtained via the ICES data repository were collected as part of the Tracer and Circulation in the Nordic Seas Region (TRACTOR) project. We are very grateful to Kelly K. Falkner who was supported by funding from the U.S. National Science Foundation, Office of Polar Programs (NSF #0230354), and acknowledge the provision of nutrient data from the Canadian Archipelago Throughflow Study Project (CATS, at http://www.udel.edu/CAT). We are also very grateful to Andrey Proshutinsky and Eddy Carmack, and acknowledge the provision of nutrient data from the Beaufort Gyre, collected and made available by the Beaufort Gyre Exploration Project based at the Woods Hole Oceanographic Institution (http://www.whoi.edu/beaufortgyre) in collaboration with researchers from Fisheries and Oceans Canada at the Institute of Ocean Sciences. Likewise, we are also grateful to Craig Lee and acknowledge the provision of data through the Freshwater Initiative-Davis Strait Program supported by NSF-OPP grants OPP0230381 and OPP0632231. Some plots were produced using the Ocean Data View software (Schlitzer, R., Ocean Data View, http://www.odv.awi.de, 2012). We thank Eleanor Frajka-Williams (NOCS, UK) for constructive discussions. An earlier version of the manuscript benefited from the comments by Stuart Painter, Stephanie Henson, and Mark Stinchcombe (NOCS, UK). We are very grateful to three anonymous reviewers for their constructive comments, suggestions, and criticisms which helped strengthen this manuscript.

References

Agnew, T., A. Lambe, and D. Long (2008), Estimating sea ice area flux across the Canadian Arctic Archipelago using enhanced AMSR-E, *J. Geophys. Res.*, *113*(C10), C10,011, doi:10.1029/2007JC004582.

Aminot, A., R. Kérouel, and S. C. Coverly (2009), Nutrients in Seawater Using Segmented Flow Analysis, in *Practical Guidelines for the Analysis of Seawater*, edited by O. Wurl, pp. 143–178, CRC Press, Boca Raton, Fla.

Anderson, L. G., D. W. Dyrssen, E. P. Jones, and M. G. Lowings (1983), Inputs and outputs of salt, fresh water, alkalinity, and silica in the Arctic Ocean, *Deep Sea Research A*, *30*(1), 87–94, doi:10.1016/0198-0149(83)90036-5.

Anderson, L. G., E. P. Jones, and J. H. Swift (2003), Export production in the central Arctic Ocean evaluated from phosphate deficits, *J. Geophys. Res.*, *108*, C6, doi: 10.1029/2001JC001057.

Arrigo, K. R., G. V. Dijken, and S. Pabi (2008), Impact of a shrinking Arctic ice cover on marine primary production, *Geophys. Res. Lett.*, *35*, L19603, doi:10.1029/2008GL035028.

Azetsu-Scott, K., and P. Yeats (2007), Changing chemical environment in the Labrador Sea: consequences for climate and ecosystem studies, *AZMP Bulletin PMZA*, *6*, 16–19.

Björkman, K. M., and D. M. Karl (2003), Bioavailability of dissolved organic phosphorus in the euphotic zone at Station ALOHA, North Pacific Subtropical Gyre, *Limnology And Oceanography*, *48*(3), 1049–1057, doi:10.4319/lo.2003.48.3.1049.

Blais, M., J.-E. Tremblay, A. D. Jungblut, J. Gagnon, J. Martin, M. Thaler, and C. Lovejoy (2012), Nitrogen fixation and identification of potential diazotrophs in the Canadian Arctic, *Global Biogeochem. Cycles*, doi:10.1029/2011GB004096.

Bouwman, A. F., G. V. Drecht, J. M. Knoop, A. H. W. Beusen, and C. R. Meinardi (2005), Exploring changes in river nitrogen export to the world's oceans, *Global Biogeochem. Cycles*, *19*, doi:10.1029/2004GB002314.

Budéus, G., E. Fahrbach, and P. Lemke (2008), The Expedition ARKTIS-XXI/1 a and b of the Research Vessel Polarstern in 2005. Reports on Polar and Marine Research, Alfred Wegener Institute for Polar and Marine Research, Bremerhaven, 570, 145 pp, hdl:10013/epic.30795.d001, Tech. rep., Alfred Wegener Institute for Polar and Marine Research.

Cai, P., M. Rutgers van der Loeff I., Stimac, E.M. Nöthig, K. Lepore, and S. B. Moran (2010), Low export flux of particulate organic carbon in the central Arctic Ocean as revealed by ^{234}Th:^{238}U disequilibrium, *J. Geophys. Res.*, *115*, C10037, doi:10.1029/2009JC005595.

Chang, B. X., and A. H. Devol (2009), Seasonal and spatial patterns of sedimentary denitrification rates in the Chukchi Sea, *Deep Sea Research II*, *56*, 1339–1350, doi:10.1016/j.dsr2.2008.10.024.

Clark, L. L., E. D. Ingall, and R. Benner (1998), Marine phosphorus is selectively remineralized, *Nature*, *393*.

Coachman, L. K., and K. Aagaard (1974), *Physical oceanography of the Arctic and Subarctic Seas, in* Marine Geology and Oceanography of the Arctic Seas. Edited by Y. Herman, pp. 1–72, Springer-Verlag, New York, N. Y.

Codispoti, L. A., and D. Lowman (1973), A reactive silicate budget for the Arctic Ocean, *Limnology And Oceanography*, *18(3)*, 448.

Codispoti, L. A., and T. G. Owens (1975), Nutrient transports through Lancaster Sound in relation to the Arctic Ocean's reactive silicate budget and the outflow of Bering Strait waters, *Limnology And Oceanography*, *20*(1), pp. 115–119.

Codispoti, L. A., C. N. Flagg, and J. H. Swift (2009), Hydrographic conditions during the 2004 SBI process experiments, *Deep-Sea Res.* II, *56*(17), 1144–1163, doi: 10.1016/j.dsr2.2008.10.013.

Cuny, J., P. B. Rhines, F. Schott, and J. Lazier (2005), Convection above the Labrador Continental Slope, *J. Phys. Oceanogr.*, *35*(4), 489–511, doi:10.1175/JPO2700.1.

Curry, B., C. M. Lee, and B. Petrie (2011), Volume, freshwater, and heat fluxes through Davis Strait, 2004–05, *J. Phys. Oceanogr.*, *41*(3), 429–436, doi:10.1175/2010JPO4536.1.

DeMaster, D. (1981), The supply and accumulation of silica in the marine environment, *Geochimica Et Cosmochimica Acta*, *45*(10), 1715–1732, doi:10.1016/0016-7037(81)90006-5.

Deutsch, C., J. L. Sarmiento, D. M. Sigman, N. Gruber, and J. P. Dunne (2007), Spatial coupling of nitrogen inputs and losses in the ocean, *Nature*, *445*, doi:10.1038/nature05392.

Divine, D. V., and C. Dick (2006), Historical variability of sea ice edge position in the Nordic Seas, *J. Geophys. Res.*, *111*(C1), C01001, doi:10.1029/2004JC002851.

Duhamel, S., S. T. Dyhrman, and D. M. Karl (2010), Alkaline phosphatase activity and regulation in the North Pacific Subtropical Gyre, *Limnology And Oceanography*, *55*(3), 1414–1425, doi:10.4319/lo.2010.55.3.1414.

Falck, E., G. Kattner, and G. Budéus (2005), Disappearance of Pacific Water in the northwestern Fram Strait, *Geophys. Res. Lett.*, *32*, L14619, doi:10.1029/2005GL023400.

Frey, K. E., and J. W. McClelland (2009), Impacts of permafrost degradation on arctic river biogeochemistry, *Hydrol. Process.*, *23*(1), 169–182, doi:10.1002/hyp.7196.

Frey, K. E., J. W. McClelland, R. M. Holmes, and L. C. Smith (2007), Impacts of climate warming and permafrost thaw on the riverine transport of nitrogen and phosphorus to the Kara Sea, *J. Geophys. Res.*, *112*, *G4*, doi:10.1029/2006JG000369.

Ganachaud, A., and C. Wunsch (2002), Oceanic nutrient and oxygen transports and bounds on export production during the World Ocean Circulation Experiment, *Global Biogeochem. Cycles*, *16*(4), doi:10.1029/2000GB001333.

Gordon, L. I., J. C. Jennings, A. A. Ross, and J. M. Krest (1993), A suggested protocol for continuous flow automated analysis of seawater nutrients (phosphate, nitrate, nitrite and silicic acid) in the WOCE Hydrographic Program and the Joint Global Ocean Fluxes Study, *Tech. rep.*, WOCE Hydrographyc Programe Office, Methods Manual WHPO 91-1.

Grasshoff, K., K. Kremling, and M. Ehrhardt (1999), Methods of Seawater Analysis, Wiley-VCH Verlag GmbH, Weinheim, Germany.

Hodson, A., A. Gurnell, M. Tranter, J. Bogen, J. Hagen, and M. Clark (1998), Suspended sediment yield and transfer processes in a small High-Artic glacier basin, Svalbard, *Hydrol. Process.*, *12* (1), 73–86.

Hodson, A., P. Mumford, J. Kohler, and P. Wynn (2005), The High Arctic glacial ecosystem: new insights from nutrient budgets, *Biogeochemistry*, *72*(2), 233–256, doi:10.1007/s10533-004-0362-0.

Holmes, R. M., J. W. McClelland, B. J. Peterson, S. E. Tank, E. Bulygina, T. I. Eglinton, V. V. Gordeev, T. Y. Gurtovaya, P. A. Raymond, D. J. Repeta, R. Staples, R. G. Striegl, A. V. Zhulidov, and S. A. Zimov (2011), Seasonal and annual fluxes of nutrients and organic matter from large rivers to the Arctic Ocean and surrounding seas, *Estuaries and Coasts*, doi:10.1007/s12237-011-9386-6.

Honjo, S., R. A. Krishfield, T. I. Eglinton, S. J. Manganini, J. N. Kemp, K. Doherty, J. Hwang, T. K. McKee, and T. Takizawa (2010), Biological pump processes in the cryopelagic and hemipelagic Arctic Ocean: Canada Basin and Chukchi Rise, *Progress In Oceanography*, *85*, 137–170, doi:10.1016/j.pocean.2010.02.009.

Jensen, L. M., and M. Rasch (2008), Nuuk Ecological Research Operations, 1st Annual Report, 2007, *Tech. rep.*, Danish Polar Centre, Danish Agency for Science, Technology and Innovation, Ministry of Science, Technology and Innovation, Copenhagen.

Jones, E. P., and A. R. Coote (1980), Nutrient distributions in the Canadian Archipelago: Indicators of summer water mass and flow characteristics, *Can. J. Fish. Aquat. Sci.*, *37*(4), 589–599, doi:10.1139/f80-075.

Jones, E. P., D. Dyrssen, and A. R. Coote (1984), Nutrient regeneration in deep Baffin Bay with consequences for measurements of the conservative tracer NO and fossil fuel CO_2 in the oceans, *Can. J. Fish. Aquat. Sci.*, *41*(1), 30–35, doi:10.1139/f84-003.

Jones, E. P., L. G. Anderson, and J. H. Swift (1998), Distribution of Atlantic and Pacific waters in the upper Arctic Ocean: Implications for circulation, *Geophys. Res. Lett.*, *25*(6), 765–768.

Jones, E. P., J. H. Swift, L. G. Anderson, M. Lipizer, G. Civitarese, K. K. Falkner, G. Kattner, and F. McLaughlin (2003), Tracing Pacific water in the North Atlantic Ocean, *J. Geophys. Res.*, *108*, *C4*, 3116, doi:10.1029/2001JC001141.

Kanakidou, M., R. A. Duce, J. M. Prospero, A. R. Baker, C. Benitez-Nelson, F. J. Dentener, K. A. Hunter, P. S. Liss, N. Mahowald, G. S. Okin, M. Sarin, K. Tsigaridis, M. Uematsu, L. M. Zamora, and T. Zhu (2012), Atmospheric fluxes of organic N and P to the global ocean, *Global Biogeochem. Cycles*, *26*(3), GB3026, doi:10.1029/2011 GB004277.

Karl, D. M., and K. M. Björkman (2002), Dynamics of DOP, in *Biogeochemistry of Marine Dissolved Organic Matter*, edited by D. A. Hansell and C. A. Carlson, pp. 249–366, Elsevier Inc., doi:10.1016/B978-012323841-2/50008-7.

Kattner, G. (2009), Nutrients measured on water bottle samples during POLARSTERN leg ARK-XXI/1 a and b., AWI Data set, PANGEA, Data Publisher for Earth and Environmental Science at http://www.pangaea.de/, doi:10.1594/PANGEA.714254.

Kwok, R. (2006), Exchange of sea ice between the Arctic Ocean and the Canadian Arctic Archipelago, *Geophys. Res. Lett.*, *33*(16), L16,501–, doi:10.1029/2006GL027094.

Lalande, C., S. Belanger, and L. Fortier (2009a), Impact of a decreasing sea ice cover on the vertical export of particulate organic carbon in the northern Laptev Sea, Siberian Arctic Ocean, *Geophys. Res. Lett.*, *36*, L21604, doi:10.1029/2009GL040570.

Lalande, C., A. Forest, D. G. Barber, Y. Gratton, and L. Fortier (2009b), Variability in the annual cycle of vertical particulate organic carbon export on Arctic shelves: Contrasting the Laptev Sea, Northern Baffin Bay and the Beaufort Sea, *Cont. Shelf Res.*, *29*(17), 2157–2165, doi:10.1016/j.csr.2009.08.009.

Lee, C. M., J. Abriel, J. I. Gabat, B. Petrie, M. Scotney, V. Soukhovtsev, and K. V. Thiel (2004), An Observational Array for High-Resolution, Year-Round Measurements of Volume, Freshwater, and Ice Flux Variability in Davis Strait: Cruise Report for R/V Knorr 179-05, 22 September - 4 October 2004, Univ. of Washington, Seattle, WA., Tech. rep.

Loder, J. W., B. Petrie, and G. Gawarkiewicz (1998), The coastal ocean off northeastern North America: a large-scale view, in *The Global Coastal Ocean: Regional Studies and Synthesis*, edited by A. R. Robinson and K. H. Brink, pp. 105–133, John Willey and Sons, Inc., New York.

Loeng, H., V. Ozhigin, and B. Adlandsvik (1997), Water fluxes through the Barents Sea, *ICES J. Mar. Sci.*, *54*(3), 310–317, doi:10.1006/jmsc.1996.0165.

Macdonald, R. W., L. G. Anderson, J. P. Christensen, L. A. Miller, I. P. Semiletov, and R. Stein (2010), The Arctic Ocean, in Carbon and Nutrient Fluxes in Continental Margins: A Global Synthesis, edited by K.-K. Liu, L. Atkinson, R. Quiñones, and L. Talaue-McManus, pp. 291–303, Springer Berlin Heidelberg.

Macias Fauria, M., A. Grinsted, S. Helama, J. Moore, M. Timonen, T. Martma, E. Isaksson, and M. Eronen (2009), Unprecedented low twentieth century winter sea ice extent in the Western Nordic Seas since A.D. 1200, *Clim. Dyn.*, *34*(6), 781–795, doi:10.1007/s00382-009-0610-z.

Mahaffey, C., R. G. Williams, G. A. Wolff, and W. T. Anderson (2004), Physical supply of nitrogen to phytoplankton in the Atlantic Ocean, *Global Biogeochem. Cycles*, *18*(1), 1–12.

McClelland, J. W., S. J. Dery, B. J. Peterson, R. M. Holmes, and E. F. Wood (2006), A pan-Arctic evaluation of changes in river discharge during the latter half of the 20th century, *Geophys. Res. Lett.*, *33*, L06715, doi:10.1029/2006GL025753.

McLaughlin, F., A. Proshutinsky, E. C. Carmack, K. Shimada, M. Corkum, J. Eert, C. Guay, R. Krishfield, B. Li, H. Maclean, J. Nelson, W. Richardson, D. Sieberg, J. Smith, M. Steel, N. Sutherland, W. Walczowski, L. White, M. Yamamoto-Kawai, and S. Zimmermann (2010), Physical, chemical and zooplankton data from the Canada Basin and Canadian Arctic Archipelago, July 29 to September 1, 2005, *Canadian Data Report of Hydrography and Ocean Sciences*, p. 298.

McLaughlin, F. A., E. C. Carmack, Robie, W. Macdonald, and J. K. B. Bishop (1996), Physical and geochemical properties across the Atlantic/Pacific water mass front in the southern Canadian Basin, *J. Geophys. Res.*, *101*, *C1*, 1183–1197.

Melling, H., T. A. Agnew, K. K. Falkner, D. A. Greenberg, C. M. Lee, A. Munchow, B. Petrie, S. J. Prinsenberg, R. M. Samelson, and R. A. Woodgate (2008), Fresh-Water Fluxes via Pacific and Arctic Outflows Across the Canadian Polar Shelf, in *Arctic–Subarctic Ocean Fluxes*, edited by R. R. Dickson, J. Meincke, and P. Rhines, pp. 193–247, Springer Netherlands, Dordrecht, doi:10.1007/978-1-4020-6774-7_10.

Mernild, S. H., G. E. Liston, C. A. Hiemstra, K. Steffen, E. Hanna, and J. H. Christensen (2009), Greenland Ice Sheet surface mass-balance modelling and freshwater flux for 2007, and in a 1995-2007 perspective, *Hydrol. Process.*, *23*(17), 2470–2484, doi:10.1002/hyp.7354.

Michel, C., M. Gosselin, and C. Nozais (2002), Preferential sinking export of biogenic silica during the spring and summer in the North Water Polynya (northern Baffin Bay): Temperature or biological control?, *J. Geophys. Res.*, *107*, *C7*, 3064, doi:10.1029/2000JC000408.

Muench, R. D. (1970), The physical oceanography of the northern Baffin Bay region, Ph.D. thesis, University of Washington, Seattle, Wash.

Munchow, A., and H. Melling (2008), Ocean current observations from Nares Strait to the west of Greenland: Interannual to tidal variability and forcing, *Journal of Marine Research*, *66*(6), 801–833.

Pabi, S., G. L. v. Dijken, and K. R. Arrigo (2008), Primary production in the Arctic Ocean, 1998-2006, *J. Geophys. Res.*, *113*, C08005, doi:10.1029/2007JC004578.

Palter, J. B., M. S. Lozier, J. L. Sarmiento, and R. G. Williams (2011), The supply of excess phosphate across the Gulf Stream and the maintenance of subtropical nitrogen fixation, *Global Biogeochem. Cycles*, *25*(4), doi:10.1029/2010GB003955.

Peterson, B. J., R. M. Holmes, J. W. McClelland, C. J. Vorosmarty, R. B. Lammers, A. I. Shiklomanov, and I. A. S. S. Rahmstorf (2002), Increasing river discharge to the Arctic Ocean, *Science*, *298*, 2171–2173.

Peterson, B. J., J. McClelland, R. Curry, R. M. Holmes, W. Je, and K. Aagaar (2006), Trajectory shifts in the Arctic and Subarctic freshwater cycle, *Science*, *313*, 1061–1066, doi:10.1126/science.1122593.

Prinsenberg, S., J. Hamilton, I. Peterson, and R. Pettipas (2009), Observing and interpreting the seasonal variability of the oceanographic fluxes passing through Lancaster Sound of the Canadian Arctic Archipelago, in NATO Science for Peace and Security Series C: Environmental Security, edited by J. C. J. Nihoul and A. G. Kostianoy, pp. 125–143, Springer Netherlands, Dordrecht, doi:10.1007/978-1-4020-9460-6_10.

Rabe, B., A. M., Unchow, H. L. Johnson, and H. Melling (2010), Nares Strait hydrography and salinity field from a 3-year moored array, *J. Geophys. Res.*, *115*, C07010, doi:10.1029/2009JC005966.

Raimbault, P., N. Garcia, and F. Cerutti (2008), Distribution of inorganic and organic nutrients in the South Pacific Ocean - evidence for long-term accumulation of organic matter in nitrogen-depleted waters, *Biogeosciences*, *5*, 281–298.

Raymond, P. A., J. W. McClelland, R. M. Holmes, A. V. Zhulidov, K. Mull, B. J. Peterson, R. G. Striegl, G. R. Aiken, and T. Y. Gurtovaya (2007), Flux and age of dissolved organic carbon exported to the Arctic Ocean: A carbon isotopic study of the five largest arctic rivers, *Global Biogeochem. Cycles*, *21*(4), doi:10.1029/2007GB002934.

Roemmich, D. (1983), Optimal estimation of hydrographic station data and derived fields, *J. Phys. Oceanogr.*, *13*, 1544–1549, doi:10.1175/1520-0485(1983)013<1544:OEOHSD>2.0.CO;2.

Roussenov, V., R. G. Williams, C. Mahaffey, and G. A. Wolff (2006), Does the transport of dissolved organic nutrients affect export production in the Atlantic Ocean?, *Global Biogeochem. Cycles*, *20*, GB3002, doi:10.1029/2005GB002510.

Rudels, B. (2011), Volume and freshwater transports through the Canadian Arctic Archipelago–Baffin Bay system, *J. Geophys. Res.*, *116*, C00D10, doi:10.1029/2011JC007019.

Shiklomanov, A. I., and R. B. Lammers (2009), Record Russian river discharge in 2007 and the limits of analysis, *Environ. Res. Lett.*, *4*, 045015, doi:10.1088/1748-9326/4/4/045015.

Simpson, K. G., J.-E. Tremblay, Y. Gratton, and N. M. Price (2008), An annual study of inorganic and organic nitrogen and phosphorus and silicic acid in the southeastern Beaufort Sea, *J. Geophys. Res.*, *113*, C07016, doi:10.1029/2007JC004462.

Tank, S. E., M. Manizza, R. M. Holmes, J. W. McClelland, and B. J. Peterson (2011), The processing and impact of dissolved riverine nitrogen in the Arctic Ocean, *Estuaries and Coasts*, doi:10.1007/s12237-011-9417-3.

Torres-Valdes, S., V. M. Roussenov, R. Sanders, S. Reynolds, X. Pan, R. Mather, A. Landolfi, G. A. Wolff, E. P. Achterberg, and R. G. Williams (2009), Distribution of dissolved organic nutrients and their effect on export production over the Atlantic Ocean, *Global Biogeochem. Cycles*, *23*, GB4019, doi:10.1029/2008GB003389.

Tovar-Sánchez, A., C. M. Duarte, J. C. Alonso, S. Lacorte, R. Tauler, and C. Galbán-Malagón (2010), Impacts of metals and nutrients released from melting multiyear Arctic sea ice, *J. Geophys. Res.*, *115*, C07003, doi:10.1029/2009JC005685.

Tremblay, J.-E., Y. Gratton, E. C. Carmack, C. D. Payne, and N. M. Price (2002a), Impact of the large-scale Arctic circulation and the North Water Polynya on nutrient inventories in Baffin Bay, *J. Geophys. Res.*, *107*, C8, 3112.

Tremblay, J.-E., Y. Gratton, J. Fauchot, and N. Price (2002b), Climatic and oceanic forcing of new, net, and diatom production in the North Water, *Deep Sea Research II*, *49*(22-23), 4927–4946.

Tsubouchi, T., S. Bacon, A. C. Naverira-Garabato, Y. Aksenov, S. W. Laxon, E. Fahrbach, A. Beszczynska-Möller, E. Hansen, C. M. Lee, and R. B. Ingvaldsen (2012), The Arctic Ocean in summer: a quasi-synoptic inverse estimate of boundary fluxes and water mass transformation, *J. Geophys. Res.*, doi:10.1029/2011JC007174.

Wadham, J. L., M. Tranter, M. Skidmore, A. J. Hodson, J. Priscu, W. B. Lyons, M. Sharp, P. Wynn, and M. Jackson (2010), Biogeochemical weathering under ice: Size matters, *Global Biogeochem. Cycles*, *24*, GB3025, doi:10.1029/2009GB003688.

Wunsch, C. (1996), The Ocean Circulation Inverse Problem, Cambridge University Press, New York.

Yamamoto-Kawai, M., E. Carmack, and F. McLaughlin (2006), Nitrogen balance and Arctic throughflow, *Nature*, *443*, 43.